ISSN 2457 – 5275 (Online, English)
ISSN 1842 – 4074 (Print, Online, Romanian)

September 2017
Volume 23
Number 3
4 th Series

RoJAE

Romanian Journal of Automotive Engineering

SIAR
The Journal of the Society of Automotive Engineers of Romania
www.siar.ro
www.ro-jae.ro

RoJAE

Romanian

Journal of Automotive Engineering

Societatea Inginerilor de Automobile din România
Society of Automotive Engineers of Romania
www.siar.ro

SIAR – The Society of Automotive Engineers of Romania is the professional organization of automotive engineers, an independent legal entity, non-profit, active member of FISITA (Fédération Internationale des Sociétés d'Ingénieurs des Techniques de l'Automobile - International Federation of Automotive Engineering Societies) and EAEC (European Cooperation Automotive Engineers).

Founded in January 1990 as a professional association, non-governmental, SIAR's main objectives are: development and increase the exchange of professional information, promoting Romanian scientific research results, new technologies specific to automotive industry, international cooperation.

Shortly after its constitution, SIAR was affiliated to FISITA - International Federation of Automotive Engineers and EAEC - European Conference of Automotive Engineers, thus ensuring full involvement in specific activities undertaken globally.

In order to help promoting the science and technology in the automotive industry, SIAR is issuing 4 times a year rIA - Journal of Automotive Engineers (on paper in Romanian and electronically in Romanian and English).

The organization of national and international scientific meetings with a large participation of experts from universities and research institutes and economic environment is an important part of SIAR's. In this direction, SIAR holds an annual scientific event with a wide international participation. The SIAR annual congress is hosted successively by large universities that have ongoing programs of study in automotive engineering.

Developing relationships with the economic environment is a constant concern. The presence in Romania of OEMs and their suppliers enables continuous communication between industry and academia.

Actually, a constant priority in SIAR's activity is to ensure optimal framework for collaboration between universities and research, industry and business specialists.

SIAR – Society of Automotive Engineers of Romania is member of:

FISITA - International Federation of Automotive Engineers Societies
www.fisita.com

EAEC - European Automotive Engineers Cooperation

RoJAE
Romanian
Journal of Automotive Engineering

CONTENTS

Volume 23, Issue No. 3 **September 2017**

The RoJAE's articles are included in the ***„Ingineria automobilului"*** magazine (*ISSN 1842 – 4074*), published by SIAR in Romanian.

The articles published in *„Ingineria automobilului"* magazine are indexed by Web of Science.

Web of Science

Clarivate Analytics

RoJAE 23(3) 91 – 128 (2017)

ISSN 2457 – 5275 (Online, English)
ISSN 1842 – 4074 (Print, Online, Romanian)

The journals of SIAR are available at the website www.ro-jae.ro.

RoJAE
Romanian
Journal of Automotive Engineering

The Journal of the Society of Automotive Engineers of Romania
www.ro-jae.ro
www.siar.ro

Production office:
The Society of Automotive Engineers of Romania (Societatea Inginerilor de Automobile din România)
Universitatea „Politehnica” din Bucuresti, Facultatea de Transporturi, Splaiul Independentei Nr. 313
060042 Bucharest ROMANIA Tel.: +4.021.316.96.08 Fax: +4.021.316.96.08 E-mail: siar@siar.ro
Staff: Prof. Minu MITREA, General Secretary of SIAR

Subscriptions: Published quarterly. Individual subscription should be ordered to the Production office.
Annual subscription rate can be found at SIAR website http://www.siar.ro.
The members of the Society of Automotive Engineers of Romania receive free a printed copy of the journal (in Romanian).

ISSN 2457 – 5275 (Online, English)
ISSN 1842 – 4074 (Print, Online, Romanian)

CORRELATION ANALYSIS - A DATA ANALYSIS TOOL IN THE VEHICLE DYNAMICS MODELING PROCESS

Constantin-Ovidiu ILIE*, Marin MARINESCU, Octavian ALEXA, Daniela VOICU, Laszlo BAROTHI

Military Technical Academy, 39-49 George Coșbuc Blvd., 050141 Bucharest, Romania
(Received 31 July 2017; Revised 08 August 2017; Accepted 24 August 2017)

Abstract: *The objective of the paper is to analyze experimental data identifying the multiple correlations between different measured parameters. This is usually the previous stage of modeling a process. Multiple correlation analysis studies the simultaneous influence of two or more sizes on the resulting variable. The results provided by it are used to determine the type of patterns to be achieved In this respect we computed the coefficient of multiple correlations of many dependencies like engine torque depending on engine load and engine speed. Data were obtained by measuring the dynamic parameters of more than 10 automobiles of the same type with similar engines and different wages and mileage. The study noted the need to perform correlation analysis before developing mathematical models of vehicle dynamics.*

Key-Words: *vehicle dynamics, modeling, multiple correlation, experimental data, vehicle speed, coefficient of correlation*

1. INTRODUCTION

It was designed and applied an experimental research program to obtain a variety of data to define the dynamics of a vehicle. We used 13 Daewoo Nubira passenger cars having mileages ranging between 13500 and 115000 km. Most of the experimental data were acquired and stored in the OEM's tester "SCAN - 100". There were measured different engine or vehicle parameters like: engine angular speed, engine load, vehicle speed.
Three parameters, engine torque, engine power and fuel consumption, could not be measured using the onboard system. Nevertheless, they were computed using static characteristics of the engine that had been obtained on the test bench. Eventually, we selected 64 tests, each of them consisting of 15th parameters. All the data were saved as a tensor. Each one of the 64th tests is a vector that has 256 values. There were captured with a frequency of 10 Hz, so each test lasts approximately 26 s.
The tensor was used to issue mathematical models that describe vehicle's dynamics [2].
Correlation deals with relationships among two or more independent variables.
Using second-order statistical characteristics, simple correlation analysis evaluates temporally correlation of two different experimental data.
As tools there were used two mathematical functions: cross-correlation function and correlation coefficient.
Cross-correlation function $R_{xy}(t_1,t_2)$ is equal for every pair of randomly chosen arguments t_1 and t_2 with:

$$R_{xy}(t_1,t_2) = M\left\{\hat{X}(t_1)\hat{Y}(t_2)\right\} = \int_{-\infty}^{\infty}\int_{-\infty}^{\infty}\{x - m_x(t_1)\}\{y - m_y(t_2)\}f_2(x_1t_1; x_2t_2)dxdy \quad (1)$$

where *x(t)* and *y(t)* are random values of *X(t)* and *Y(t)* processes.
It characterizes statistical interdependence between two random processes *X(t)* and *Y(t)* at different time points, which are at τ distance each other.
If these processes are statistically independent and their mean values are equal with zero then their cross-correlation function is equal with zero.
When the mean values of the random processes is equal with zero, than cross-correlation function becomes cross-covariance function C_{xy}.

* *Corresponding author e-mail: ovidiuilie66@yahoo.com*

ISSN 2457 – 5275 (Online, English)
ISSN 1842 – 4074 (Print, Online, Romanian)

The formula of cross-correlation function for a finite discrete experimental series is:

$$R_{xy}(r \cdot \Delta t) = \frac{1}{n-r} \sum_{i=1}^{n-r} (x_i - m_x)(y_i - m_y),\ r = 0...m \tag{2}$$

where m is maximum shift, m_x is the mean of $X(t)$ and m_y is the mean of $Y(t)$ [1].
Correlation coefficient (Pearson's coefficient) for two dynamic series x and y is computed with:

$$\rho = \frac{c_{xy}(0)}{\sqrt{c_{xx}(0) c_{yy}(0)}},\ \upsilon \in [-1;1] \tag{3}$$

where $C_{xy}(0)$ is the cross-covariance function for τ=0, $C_{xx}(0)$ and C_{yy} are covariance functions for τ=0. Maximum possible correlation occur when ρ^2=1. If ρ=1 there is a perfect linear correlation; if ρ=1 there is a perfect indirect linear correlation; if 0<ρ≤1 there is a direct dependency; and if -1≤ ρ<0 there is an indirect dependency [1].

2. MULTIPLE CORRELATION

Multiple corelation analyzes simultaniously influence of two or more variables over the output variable. In this case it is used the multiple corelation coeffiecient.
It is computed for a system with two independent input variables and one output variable with (4):

$$\rho_{y-x_1;x_2} = \sqrt{\frac{\rho_{yx_1}^2 + \rho_{yx_2}^2 - 2\rho_{yx_1}\rho_{yx_2}\rho_{x_1x_2}}{1-\rho_{x_1x_2}^2}}, \tag{4}$$

where $r_{(\cdot)}$ are simple correlation coefficients of related pairs calculated with (3) [3].
Multiple correlation coefficient can be computed also, using (5) [3]:

$$\rho_{y-x_1;...x_k} = \sqrt{1 - \frac{D_{xy}}{D_y}}, \tag{5}$$

where:

$$D_{xy} = \begin{vmatrix} 1 & \rho_{yx_1} & \rho_{yx_2} & \cdots & \rho_{yx_k} \\ \rho_{x_1y} & 1 & \rho_{x_1x_2} & \cdots & \rho_{x_1x_k} \\ \rho_{x_2y} & \rho_{x_2x_1} & 1 & \ldots & \rho_{x_2x_k} \\ \ldots & \ldots & \ldots & \ldots & \ldots \\ \rho_{x_ky} & \rho_{x_kx_1} & \rho_{x_1k_2} & \cdots & 1 \end{vmatrix} \tag{6}$$

and

$$D_y = \begin{vmatrix} 1 & \rho_{x_1x_2} & \rho_{x_1x_3} & \cdots & \rho_{x_1x_k} \\ \rho_{x_2x_1} & 1 & \rho_{x_2x_3} & \cdots & \rho_{x_2x_k} \\ \rho_{x_3x_1} & \rho_{x_3x_2} & 1 & \ldots & \rho_{x_3x_k} \\ \ldots & \ldots & \ldots & \ldots & \ldots \\ \rho_{x_kx_1} & \rho_{x_kx_2} & \rho_{x_1k_3} & \cdots & 1 \end{vmatrix} \tag{7}$$

ISSN 2457 – 5275 (Online, English)
ISSN 1842 – 4074 (Print, Online, Romanian)

Since the symmetrical coefficients of simple correlation are equal, the two determinants are symmetrical to the main diagonal.
Figure 1 presents relative (current values are divided by maximum value) cross-correlation functions and correlation coefficients of dependences: engine torque, M_e - engine load, ξ; engine torque, M_e - engine angular speed, *n;* and engine angular speed, *n* - engine load, ξ fort test *I15n*.
Also, there was noted the value of multiple correlation coefficient of engine torque, M_e as resultant parameter of engine angular speed, *n* and engine load, ξ as factorial parameters.
As can be seen, multiple correlation coefficient is greater than all simple correlation coefficients, so linearity of dependency improves using more factorial parameters.
A similar conclusion as in case of figure 1 can be drawn from figure 2 in case of dependences: vehicle speed, *V* - engine load, ξ; vehicle speed, *V* - engine angular speed, *n* and engine angular speed, *n* - engine load, ξ.

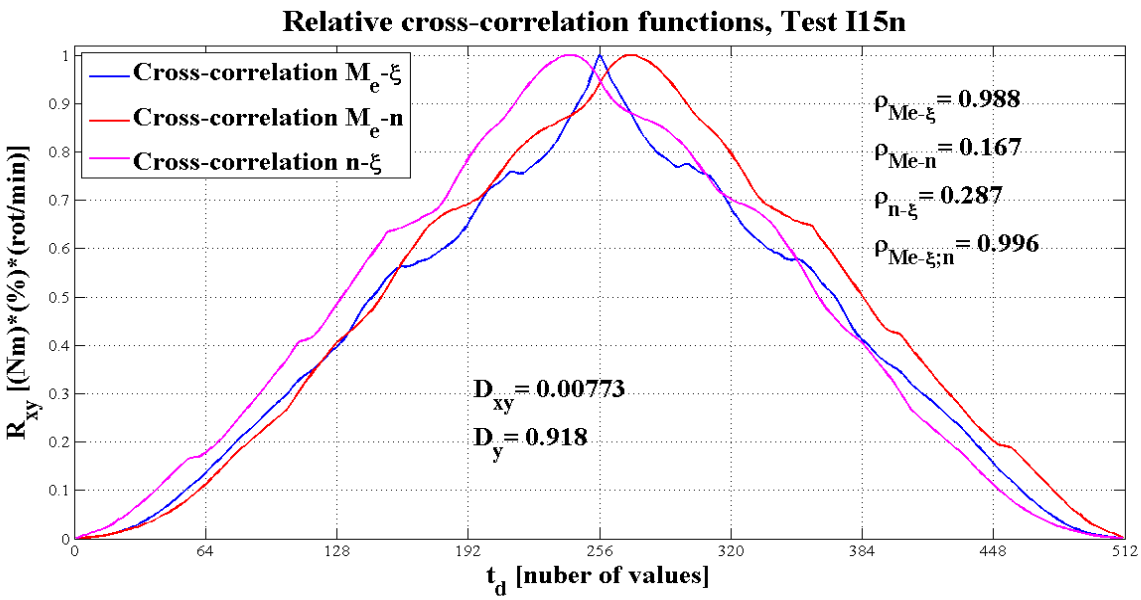

Figure 1. Relative cross-correlation functions, Test I15n

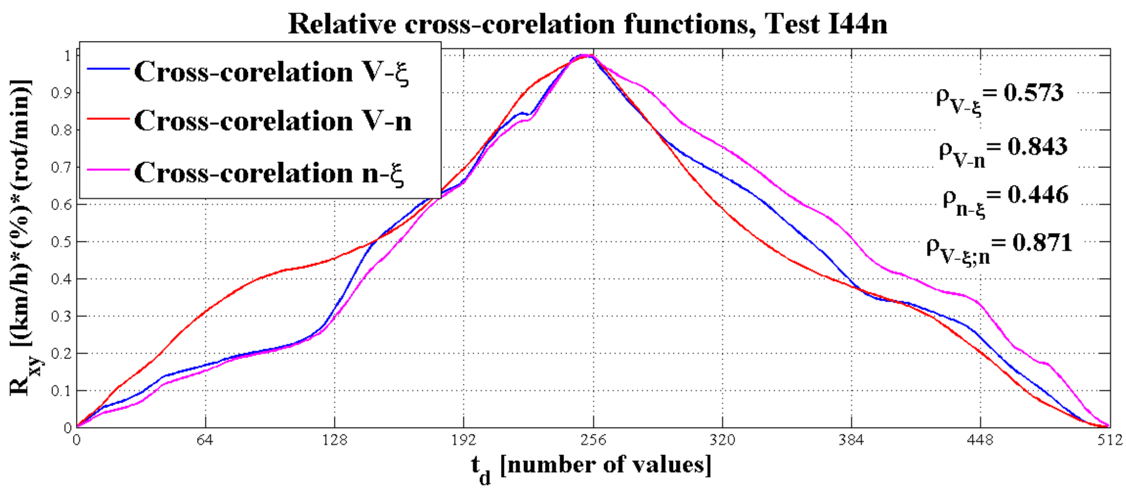

Figure 2. Relative cross-correlation function, Test I44n

In Table 1, figure 3, figure 4 and figure 5 are presented relative (current values are divided by maximum value) cross-correlation functions of all tests of vehicle speed, *V* and engine load, ξ; engine angular speed, *n* and engine load, ξ; vehicle speed, *V* and engine angular speed, *n*.
There were computed simple and multiple correlation coefficients of these dependences.
In this case multiple correlation coefficient is equal with the highest simple correlation coefficient (vehicle speed, *V* and engine angular speed, *n*).

 ISSN 2457 – 5275 (Online, English)
ISSN 1842 – 4074 (Print, Online, Romanian)

Table 2, figure 6, figure 7 and figure 8 had the same structure with figure 3, figure 4, figure 5 and Table 1. There are presented relative cross-correlation functions of all tests of engine torque, M_e and engine load, ξ; engine angular speed, n and engine load, ξ; engine torque, M_e and engine angular speed, n and multiple and simple correlation coefficients.
This time, multiple correlation coefficient is the highest and almost equal with one, that means an almost perfect correlation.
Linear nature of the dependency V=f(ξ,n) is improved adding hourly fuel consumption-C_h as factorial parameter (8).

$$\rho_{V-n,\xi,Ch} = 0{,}754 > 0{,}727 = \rho_{V,\xi,n} \tag{8}$$

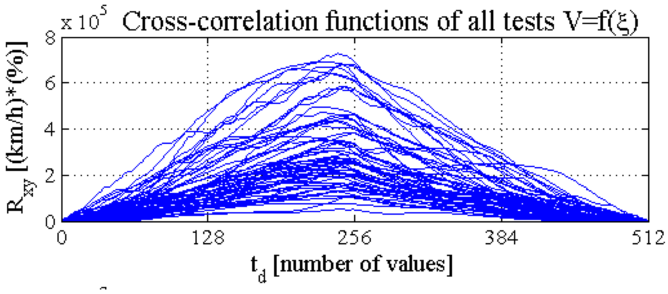

Figure 3. Relative cross-correlation functions of all tests, V=f(ξ)

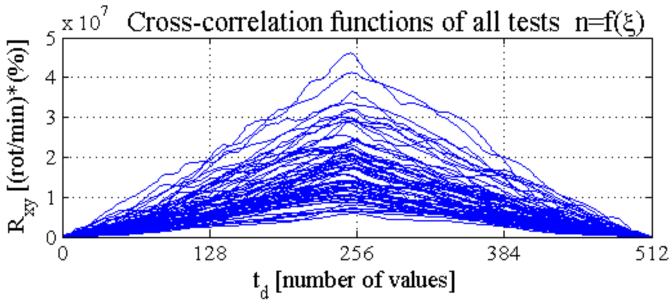

Figure 4. Relative cross-correlation functions of all tests, n=f(ξ)

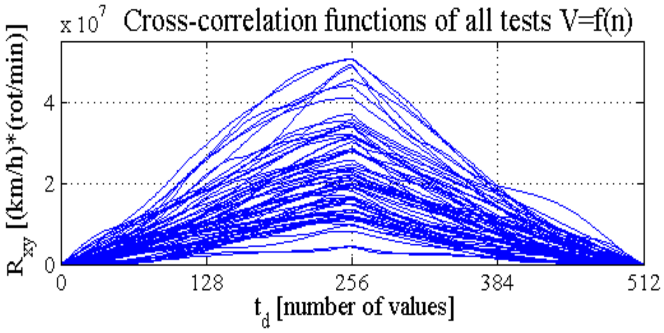

Figure 5. Relative cross-correlation functions of all tests, V=f(n)

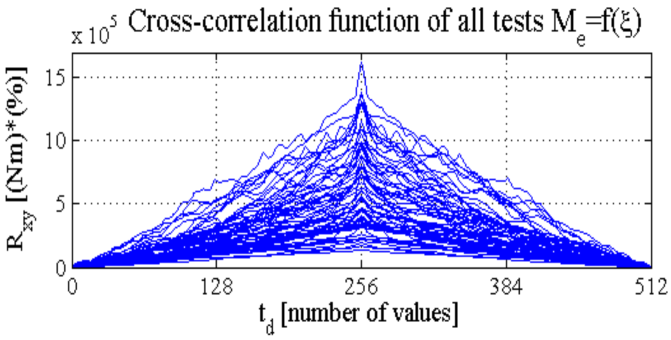

Figure 6. Relative cross-correlation functions of all tests, M_e =f(ξ)

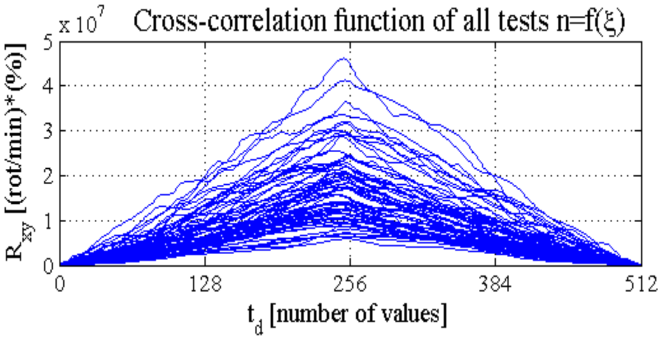

Figure 7. Relative cross-correlation functions of all tests, n=f(ξ)

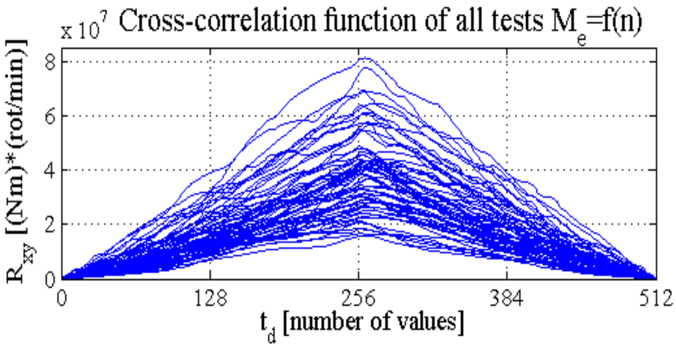

Figure 8. Relative cross-correlation functions of all tests, M_e =f(n)

Table 1.
Correlation coefficients of V=f(n, ξ) model

Correlation coefficient	$\rho_{V-\xi}$	ρ_{V-n}	$\rho_{n-\xi}$	$\rho_{V-\xi,n}$
Value	0,305	0,727	0,432	0,727

Table 2.
Correlation coefficients of M_e=f(n, ξ) model

Correlation coefficient	$\rho_{Me-\xi}$	ρ_{Me-n}	$\rho_{n-\xi}$	$\rho_{Me-\xi,n}$
Value	0,305	0,727	0,432	0,727

ISSN 2457 – 5275 (Online, English)
ISSN 1842 – 4074 (Print, Online, Romanian)

Table 3, figure 9 and figure10 revels that the best correlation is between hourly fuel consumption, C_h and engine load, ξ, respectively 0,938.
It is natural to be so because any action on the gas pedal means extra fuel sent into the combustion chamber. The correlation coefficient of hourly fuel consumption, C_h as resultant parameter and engine load, ξ as factorial parameter, $\rho_{Ch\text{-}\xi}$ is higher than multiple correlation coefficient of the model vehicle speed as resultant parameter and engine load, ξ, engine angular speed, n and hourly fuel consumption, C_h as factorial parameters, $V=f(\xi,n,C_h)$ because between vehicle speed and engine load is a weak correlation. That proves that before the designing models structure must be done a correlation analysis.
In this respect, figure 11 and Table 4 argues that adding more data to the model will not always improve the linearity of its nature so, it is possible that patterns obtained through mediation have a lower degree of precision.

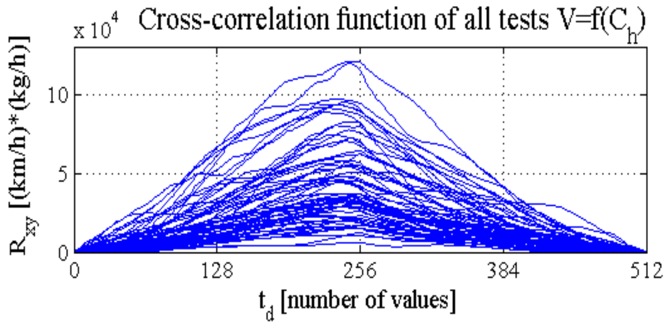

Figure 9. Relative cross-correlation functions of all tests, $V=f(C_h)$

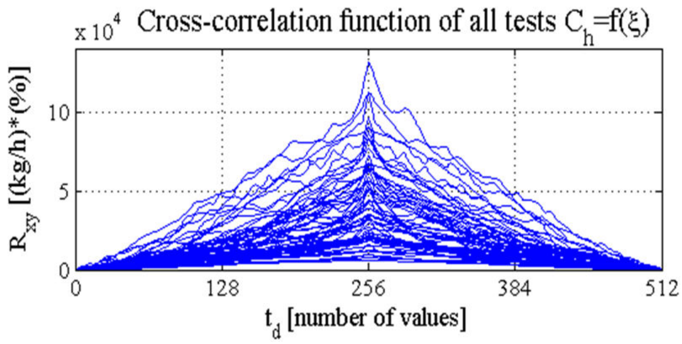

Figure 10. Relative cross-correlation functions of all tests, $C_h =f(\xi)$

Table 3.
Correlation coefficients of $V=f(\xi,n,C_h)$ model

Correlation coefficient	$\rho_{V\text{-}\xi}$	$\rho_{V\text{-}n}$	$\rho_{V\text{-}Ch}$	$\rho_{n\text{-}\xi}$
Value	0,305	0,727	0,446	0,432
Correlation coefficient	$\rho_{Ch\text{-}n}$	$\rho_{Ch\text{-}\xi}$	$\rho_{V\text{-}n,\xi,Ch}$	
Value	0,673	0,938	0,754	

Table 4.
Correlation coefficients of different parameters and tests

Correlation coefficient	16 tests	32 tests	48 tests	64 tests
M_e-ξ	0,976	0,984	0,997	0,995
M_e-n	0,325	0,220	0,324	0,321
V-ξ	0,092	0,087	0,185	0,279
V-n	0,495	0,579	0,725	0,551

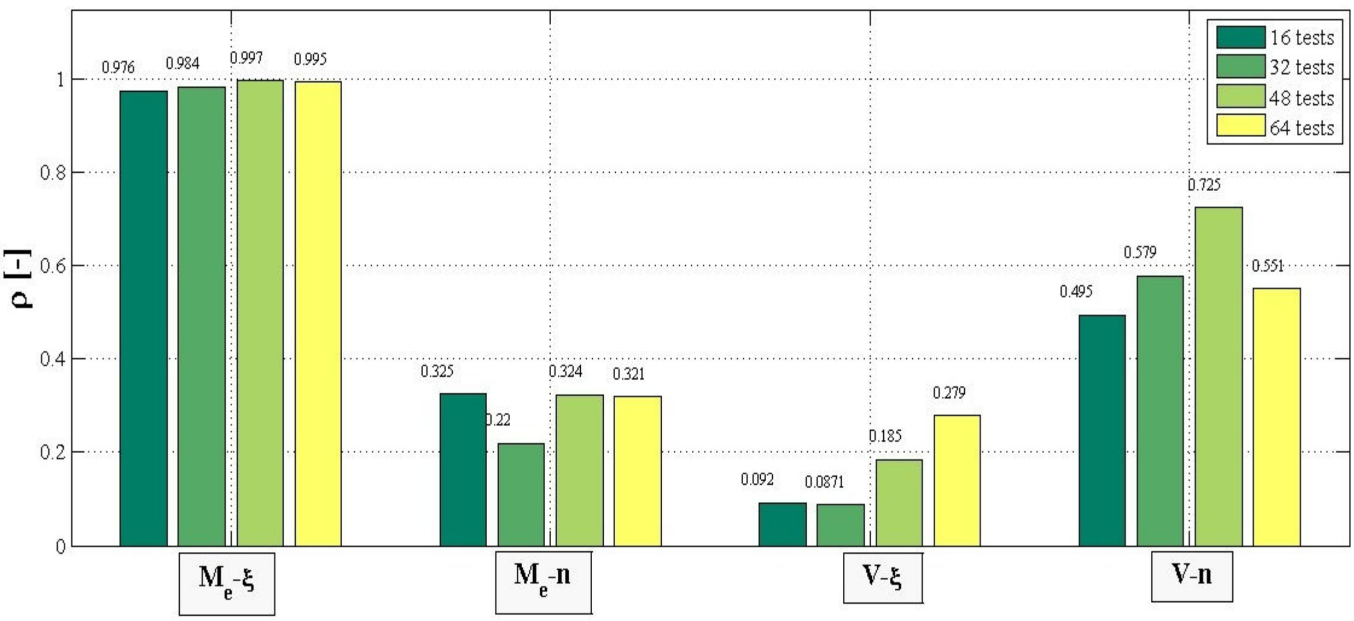

Figure 11. Correlation coefficients of different parameters and tests

ISSN 2457 – 5275 (Online, English)
ISSN 1842 – 4074 (Print, Online, Romanian)

There are presented correlation coefficients of engine torque, M_e as resultant parameter and engine load, ξ as factorial parameter; engine torque, M_e as resultant parameter and engine angular speed, *n;* vehicle speed, *V* and engine load, ξ as factorial parameter; and vehicle speed, *V* and engine angular speed *n*, models for 16, 32, 48 and 64 tests.
The correlation coefficients do not increase continuously by adding more data in the model.
This phenomenon is due to the random elements on traffic conditions that affects vehicle dynamics.
The best correlation seems to be between engine torque, M_e and engine load, ξ. A relatively good correlation shows dependence between vehicle speed, *V* and engine angular speed, *n.* The other two pairs of parameters presented show a weak connection, so accurate statistical models should be develop for engine torque, M_e - engine load, ξ and vehicle speed, *V* - engine angular speed, *n*.

3. CONCLUSION

Correlation analysis is a very important tool of analyzing statistical data. Designing accurate statistical models of vehicle dynamics is a laborious process. It requires determining the structure (patern) of the models and the minimum amount of data. The structure of the model is defined by the number of input sizes and what are they and what are the output sizes. Correlation analysis is the main mathematical tool that helps this modeling phase. It is a way to get good results during the preparing the database and the structure of models.

REFERENCES

[1] Gârlașu, S., *Introducere în analiza spectrală şi de corelaţie.* Editura Facla. Timişoara. 1982
[2] Ilie, Constantin-Ovidiu, *Modelarea statistică a dinamicii autovehiculelor.* Editura Academiei Tehnice Militare. Bucureşti. 2008
[3] Quinquis, A.; Șerbănescu, A,; Rădoi, E., *Semnale şi sisteme.* Editura Academiei Tehnice Militare. Bucureşti. 1998

ISSN 2457 – 5275 (Online, English)
ISSN 1842 – 4074 (Print, Online, Romanian)

INFLUENCE OF AERODYNAMIC ADD-ON DEVICES ON AERODYNAMIC PERFORMANCE OF AN AUTOMOBILE: A NUMERICAL STUDY

Nakka Venkata Swamy KALYAN[1)], Dipen Kumar RAJAK[2)*], Lakshmi Annamalai KUMARASWAMIDHAS[3)]

[1)] Infosys Limited, Chennai – 603002 TN, India
[2)] Department of Mechanical Engineering, Sandip Institute of Technology & Research Centre, Nashik – 422213 MH, India
[3)] Department of Mining Machinery Engineering, Indian Institute of Technology, Dhanbad – 826004 JH, India

(Received 17 May 2017; Revised 15 June 2017; Accepted 10 July 2017)

Abstract: *Aerodynamic performance is a very important criterion for an automobile, as the body design and sub-system specifications of the automobile depends on it and the performance indices like drag reduction, fuel consumption, acceleration, top speed, downward forces, skin friction and toppling moments are also influenced. The design of automotive body is primarily based on the purpose of the vehicle and the optimization of body design enhances the performance for fastback, sports and super cars. Usually sports cars implement aerodynamic add-on devices like wings/spoilers, diffusers and roof scoops, for improving the aerodynamic performance. In the present study, a numerical investigation is performed using CFD for analyzing the aerodynamic performance of a conceptual sports car and three configurations of it with aerodynamic add-on devices. The simulations results are utilized for design modifications and selection of the aerodynamic add-on devices which improve the aerodynamic performance*

Key-Words: *Aerodynamics, CFD, Automotive,Aerodynamic add-ons, Drag and Lift.*

1. INTRODUCTION

The aerodynamic performance of an automobile plays a key role in achieving the requirements according to the purpose of the vehicle. The enhancement of aerodynamic performance helps in reducing the usage of energy and also protecting the environment, which in turns results in reduction of fuel consumption, drag force and friction and increases acceleration and top speed.
It is basically influenced by the forces and moments created due to the external flow of air at the vehicle body walls [1].
The performance characteristics of aerodynamics, like drag and lift are optimized for improvement of either speed or fuel efficiency. Drag is basically the force acting on the frontal area of the automobile while the vehicle is moving forward and Lift is the resultant force created by the pressure difference between the top and bottom of the vehicle and in general these drag and lift are expressed as Coefficient of drag, C_d and lift, C_l respectively.
The optimization of drag and lift for better aerodynamic performance of the vehicle is achieved by streamlining of vehicle body and by implementing aerodynamic add-on devices like wings/spoilers, diffusers, roof scoops, under trays and wheel skirts [2][3].
Studies for improving the aerodynamic performance can be conducted either experimentally, using wind tunnels or numerically, by performing CFD analysis on the car model, with modelled boundary conditions.
For cost and time effective studies, numerical simulations are best preferred and these are also helpful in the selection of appropriate aerodynamic add-ons to the vehicle for improving the aerodynamic performance of the vehicle, when compared to wind tunnel experiment which results in great cost of both money and time.

* *Corresponding author e-mail:* dipen.pukar@gmail.com

ISSN 2457 – 5275 (Online, English)
ISSN 1842 – 4074 (Print, Online, Romanian)

CFD is basically analysing the systems associated with heat transfer, fluid flow and chemical reactions using computer simulations [4] and has its applications in industrial and non-industrial applications.
The prime applications of CFD involves in the analysis of laminar, turbulent, single phase and multi-phase flows, diffusion, reaction mechanism, phase transfer, convection, radiation and conduction [5].
CFD has been an ally to engineers since late 20th century, for modelling, studying and extemporizing many complex concepts in both cost and time effective way [6-9].
Many researchers performed simulations in CFD for analysing and understanding the aerodynamics in various fields [10-23].
In automotive industry, CFD has very huge area of application, which includes aerodynamics, cooling of engine and environment control and also implemented in product design, for cost and cycle time effectiveness and for better testing and validation of the design [24].
The flow of air around the vehicle, is basically incompressible and turbulent in nature and there are many analytical models available for modelling turbulent flow of a fluid, like Mixing length model, Spalart-Allmaras model, k-ε model, k-ω model, Algebraic stress model and Reynolds stress model, but most commonly used model for aerodynamics of automobile is standard k-ε model. Many works, like reviews and researches, related to CFD analysis of aerodynamics of an automobile are performed by numerous people [25-40].
Rizal E. M. Nasir et al. [41] studied the aerodynamics of a ARTeC's EMo-C car to determine its drag, lift and external flow around the car body, which implemented a formula car design and also performed wind tunnel experiment for validation.
The results showed a drag coefficient of 0.42 and 0.48 for CFD simulation and wind tunnel data respectively and stated that the variation in this value is due to modelling of inviscid flow in CFD, which excludes skin friction.
Johannes D. Wojciak [42] performed a detailed study on the stability and aerodynamic response of a vehicle in crosswind gusts, using CFD simulations as well as wind tunnel experiments.
It was observed that the load transients of both simulation and experiment were in good agreement with each other but whereas the simulation results of surface distribution fail at the rear-end of the vehicle and for obtaining accurate results, the ground clearance should be near to realistic values and also by maintaining a flat or symmetric under floor of the vehicle.In the present work, a conceptual design of a generic sports car is prepared and studied its aerodynamic performance of drag, lift and flow characteristics through CFD analysis.
Further study is conducted on the conceptual sports car for reducing its drag and increasing the downward force on the vehicle by implementing rear-end wing, front-end wing and rear-end diffuser.
A detailed study on the flow paths, vortices, Reynolds number and other flow and surface characteristics is conducted and compared between the four configurations for evaluating the aerodynamic performances of all the configurations of generic sports car.

2. ANALYSIS METHODOLOGY

The design of the generic sports car is done strictly using the conceptual principles, by characterising length, breadth, width, ground clearance and tire properties like wheel diameter and width, front and rear-end wheel tracks and wheel base, for the vehicle.
After the design is prepared, it is streamlined by giving edge fillets at the required positions and dimensions. Later, aerodynamic add-ons are prepared also designed and are implemented on the basic design, in order to improve the aerodynamic performance.
The rear-end wing is designed by characterising the parameters like chord, attack angle, camber height and span and the front-end wing is constructed by taking the camber line of the rear-end wing as the surface boundary and the diffuser is designed with the characterisation of fin width and flow width. Different configurations of this generic car are prepared by implementing the aerodynamic add-on devices designed and are analysed in CFD for studying their aerodynamic performance.

2.1. Design of car and accessories

The design of the sports car is completely a new and conceptual one, which is inspired by many concept car designs proposed by different automotive industries.
In the design, the hood part of the car is completely excluded and is given a fastback configuration.
The general dimensions of the basic design of the conceptual sports car (CSC) are tabulated in Table 1.

ISSN 2457 – 5275 (Online, English)
ISSN 1842 – 4074 (Print, Online, Romanian)

Table 1.
Dimensions of basic design of CSC

Parameter of the car	Dimension (mm)
Length	4800
Breadth	1800
Height	1300
Ground clearance	200
Wheel diameter	720
Wheel width	300
Front wheel track	1840
Rear wheel track	1920
Wheel base	2900

The basic design of CSC is considered as the first configuration and is therefore named as CSC-1, for convenience and the projection views of CSC-1 are shown in Figure 1.

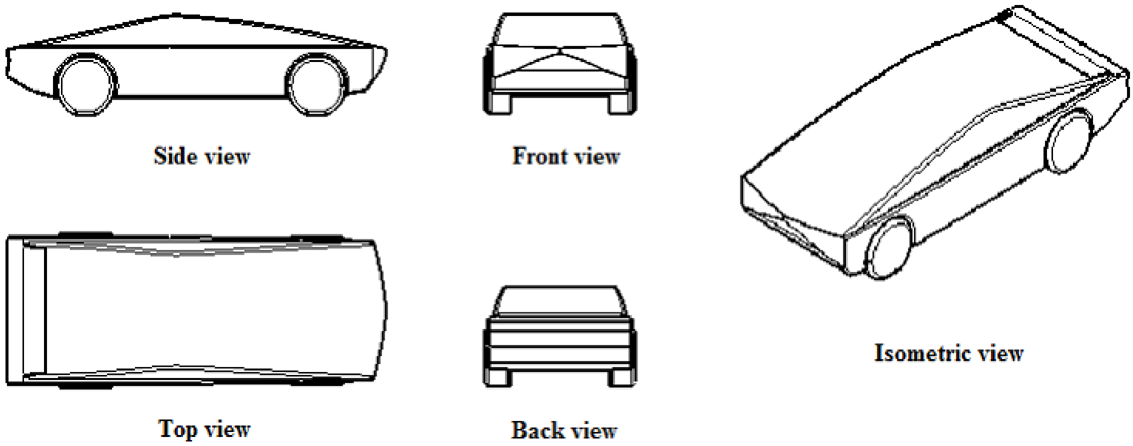

Figure 1. Projections of CSC-1

Later, three other configurations of the CSC-1 are prepared by implementing aerodynamic add-ons, i.e. rear-end wing, front-end wing and rear-end diffuser, for enhancing the aerodynamics performance of CSC-1. The aerodynamic add-ons implemented on CSC-1 are also completely new and conceptual and the generic designs of these aerodynamic add-on devices are shown in Figure 2.

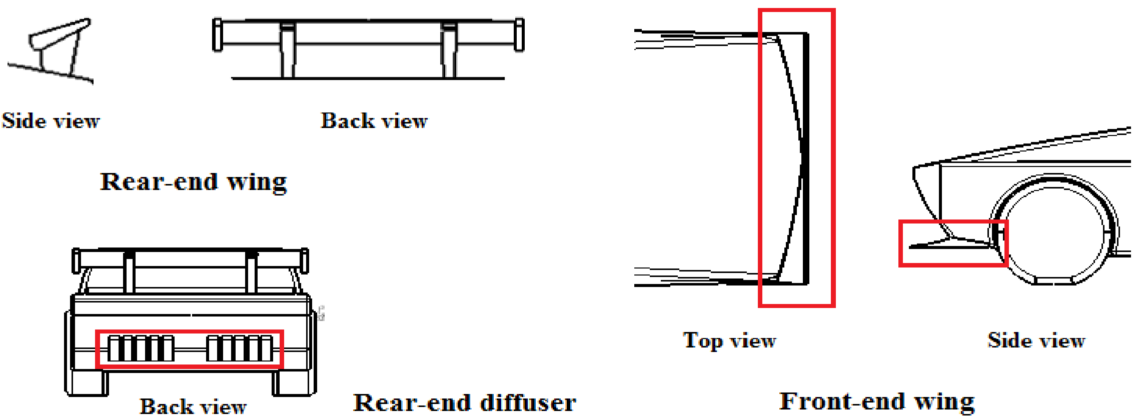

Figure 2. Generic designs of aerodynamic add-ons

ISSN 2457 – 5275 (Online, English)
ISSN 1842 – 4074 (Print, Online, Romanian)

The three configurations of CSC-1 with aerodynamic add-on devices are named as CSC-2, CSC-3 and CSC-4. The aerodynamic add-on added to CSC-2 is a rear-end wing (drifter or spoiler) and CSC-3 is an improvement to CSC-2 which implements rear-end wing along with a front-end wing.
The final design CSC - 4 implements a rear-end wing, front-end wing and a rear-end diffuser.
The designs of CSC-2, CSC-3 and CSC-4 are shown in Figure 3 and later analysed using CFD simulations, for studying aerodynamic performance of individual configuration of the generic sports car.

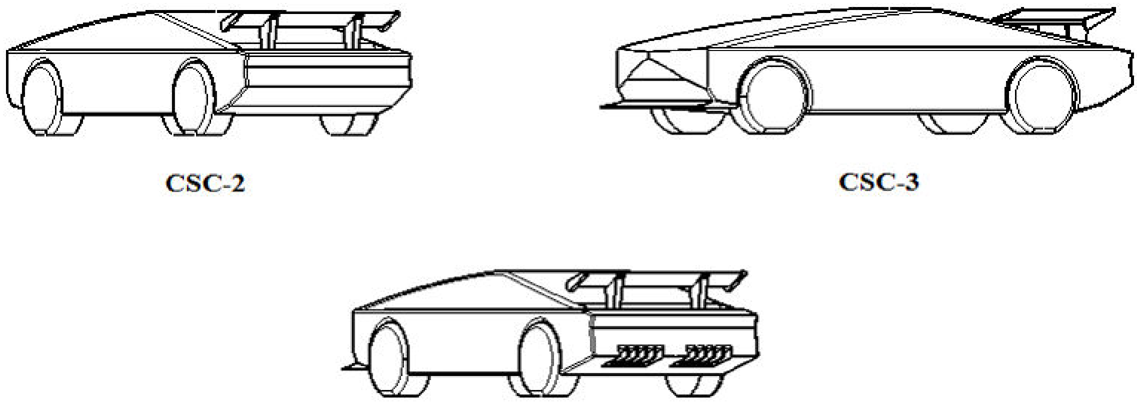

Figure 3. Configurations of Conceptual sports car with aerodynamic add-ons

2.2. CFD methodology

The aerodynamic performances of the four configurations of the generic sports car are analysed using CFD simulations, modelled for steady state turbulent fluid flow conditions, i.e. external air flow over the vehicle body, with appropriate boundary conditions of velocity inlet, pressure outlet and symmetry and stationary limits.
The CFD simulations for studying the aerodynamic performance of the four configurations of generic sports car is performed for $1/4^{th}$ model of each configuration, within a particular computational domain and used realized turbulent model and non-equilibrium wall functions for the aerodynamic analysis.
The realizable k-ε model uses the governing equations of mean flow kinetic energy and turbulent kinetic energy and k & ε equations of standard k-ε turbulent model, except that the proportionality constant in determining the eddy viscosity, C_μ is not taken as constant and is considered as a function of tensors of both rate of deformation, S_{ij} and rate of rotation, Ω_{ij}.
The computational domain is selected to be a rectangular tank covering the vehicle with dimensions proportionate to the length of the vehicle as shown in Figure 4(a).
The boundary conditions of velocity inlet are given to flow inlet plane, pressure outlet to flow outlet plane, symmetry condition for symmetry plane and stationary conditions to top plane, side plane, road and vehicle surfaces also.
The mesh required for the CFD analysis is given a fine element size, generated by program control, for obtaining efficient results of performance characteristics and is as shown in Figure 4(b), for CSC-1 and similar to CSC-1, the same program controlled fine mesh is implemented for the other configurations also.
The conditions of fluid velocity and temperature are fixed according to the Indian road conditions and environment and hence analysed for a speed of 40 m/s (144 kmph) and average temperature of 300 K (27°C). The turbulent intensity of the flow is maintained between 1-5% with a turbulent viscosity ratio of 10, which are near to the conditions of external air flow over the surface of any automobile.
The solution scheme used for performing CFD analysis is a coupled one with second order discretization for pressure, momentum, turbulent kinetic energy and rate dissipation of turbulent kinetic energy, for obtaining solution with high rate of accuracy.
The main objective is to determine the coefficient of drag and lift and other aerodynamic and surface characteristics of every configuration, for a comparative study of better aerodynamic performance, hence accuracy of the results matters a lot and therefore justifies the use of higher order conditions for the analysis.

ISSN 2457 – 5275 (Online, English)
ISSN 1842 – 4074 (Print, Online, Romanian)

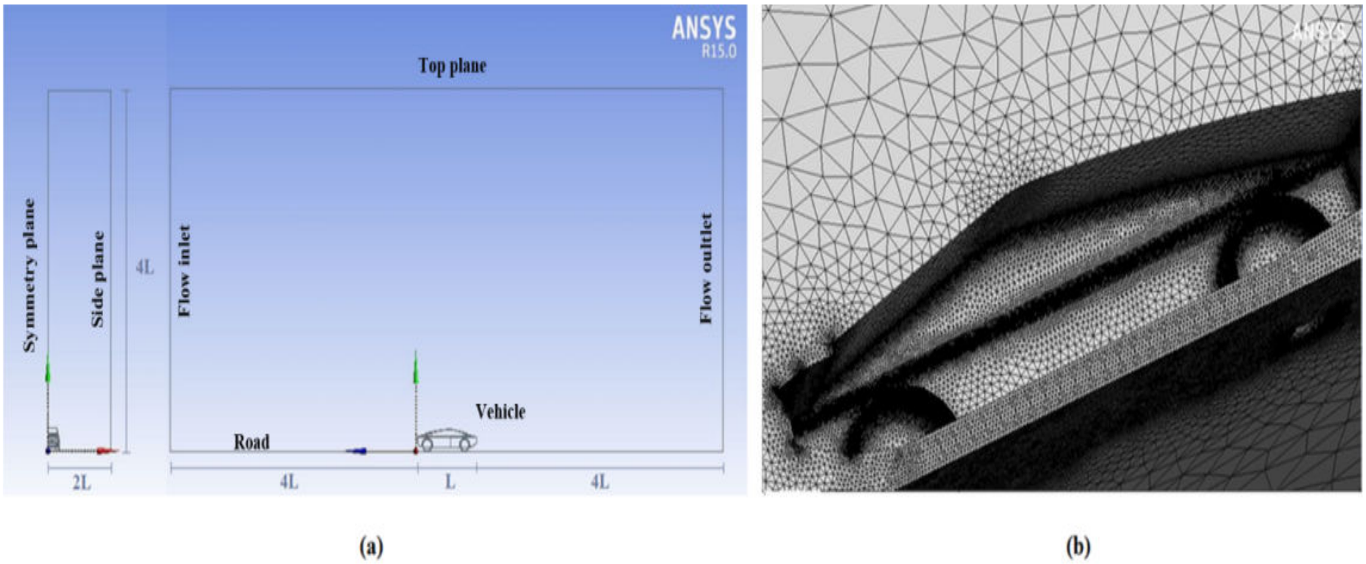

Figure 4. (a) Dimensions of CFD domain (b) Mesh of CFD analysis

The CFD analysis performed on all four configurations are of two kinds basically, 2D analysis, for understanding the flow over the boundaries of the vehicle body and 3D analysis, for complete analysis on the vehicle body, for half of the computational fluid domain as the symmetry condition exists and a complete 3D analysis is conducted on the model which has best downward force on vehicle and flow characteristics.

3. RESULTS AND DISCUSSION

The CFD analysis of 2D and 3D versions of the four configurations of generic sports car are studied in detail and the configuration which is observed to be better at aerodynamic performance is taken as the final configuration and performed a complete 3D CFD analysis on it. Initially, 2D analysis of the four configurations is performed, over the symmetry plane, to analyse the flow and turbulence energy over the boundaries of all configurations and later 3D analysis are performed over all four configurations, for a complete analysis of aerodynamic, flow and surface characteristics of all configurations of the car.

3.1. 2D CFD analysis

The initial analysis on the 2D boundary of all four configurations of car are helpful in understanding the velocity of layers of air flowing around the vehicle and the turbulent kinetic energy dissipation over the boundaries of the vehicle. It is observed that, for CSC-1 car the maximum flow velocity of air over the boundary is 60.9 m/s at the front tip of the car and the velocity ranges from 3.05 – 39.6 m/s, near to the boundaries of the vehicle.

The trailing air flow velocity, at the rear-end, varies from 12.2 – 33.5 m/s, with the least at the rear-end tip of the vehicle.

The CSC-2 has 61.7 m/s, as maximum velocity of air flow, with a velocity range of 6.17 – 37.0 m/s at near boundary of vehicle and the rear-end wing clearly splits the air flow, by increasing the flow velocity under the wing and raising the trailing air velocity and position.

The trailing air velocity lies between 24.7 – 34.0 m/s, clearly increase in the trailing velocity than CSC-1, and the position is higher and exactly back to the rear-end wing, creating a higher pressure and increasing the downward force on the vehicle.

It is observed that, there is a similar way of splitting the air flow, like CSC-2, at the rear wing in case of CSC-3, increasing the trailing air velocity and height and also observed that the same phenomenon has taken place at the front-end wing, in turn increasing the under vehicle air flow velocity.

The trailing air velocity of CSC-3 varies from 25.5 – 36.5 m/s, with a maximum flow velocity of 72.9 m/s and velocity range of 3.65 – 32.8 m/s at near boundaries.

The final configuration CSC-4 has shown a lower maximum flow velocity than CSC-3 and is 70.2 m/s.

The excess area at the bottom of rear-end due to diffuser allowed the increase of flow velocity under the vehicle at the rear-end, therefore creating lower pressure, which increased the downward force and also the flow of from under vehicle through the diffuser created an extra trailing air flow (secondary trailing air flow) and therefore due to the force of two trailing air flows, the drag of CSC-4 is reduced than CSC-3.
The velocity range of primary trailing air flow of CSC-4 is 24.6 – 42.1 m/s and that of secondary trailing air flow is 31.6 – 45.7 m/s and the velocity of air flow near the boundaries is observed to be ranging from 3.51 – 35.1 m/s.
The graphical contours representing the velocity magnitude of all four configurations of generic sports car is shown in Figure 5.

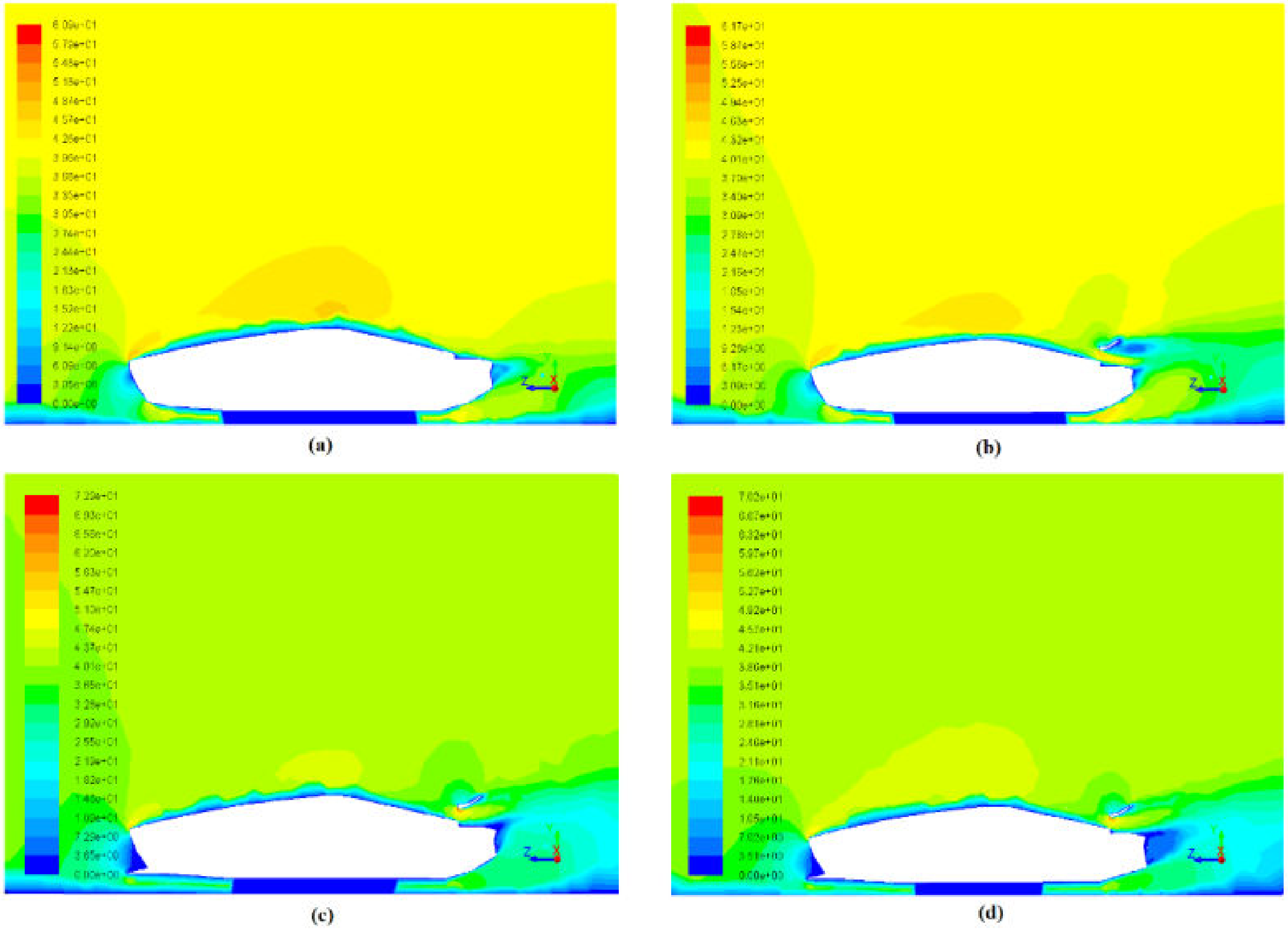

Figure 5. Velocity magnitude contours of (a) CSC-1 (b) CSC-2 (c) CSC-3 and (d) CSC-4

The turbulence energy, i.e. the turbulent kinetic energy, dissipation due to the trailing air flow at the rear-end of the vehicle for every configuration is as shown in Figure 6.
The contours clearly give sufficient support for the statements made regarding the rise in trailing air flow position and secondary trailing air flow for CSC-4.
The dissipation of turbulent kinetic energy by CSC-1 is similar to CSC-4, but lesser in area and height, which reduces the advantage of drag reduction and increasing downward force. In the case of CSC-2, as it is already stated, the downward force increases eventually, due to the position of trailing air flow.
It is observed that CSC-3 has experiencing a higher turbulent energy interaction at the front-end than CSC-4, resulting in increase in use of more energy to overcome it and evidently there will be increase in the drag on vehicle, i.e. for CSC-3.
Compared to CSC-3, CSC-4 has encountered less turbulent energy at front-end, reducing the energy consumption for overcoming the turbulent energy and eventually reducing the drag on the vehicle.

ISSN 2457 – 5275 (Online, English)
ISSN 1842 – 4074 (Print, Online, Romanian)

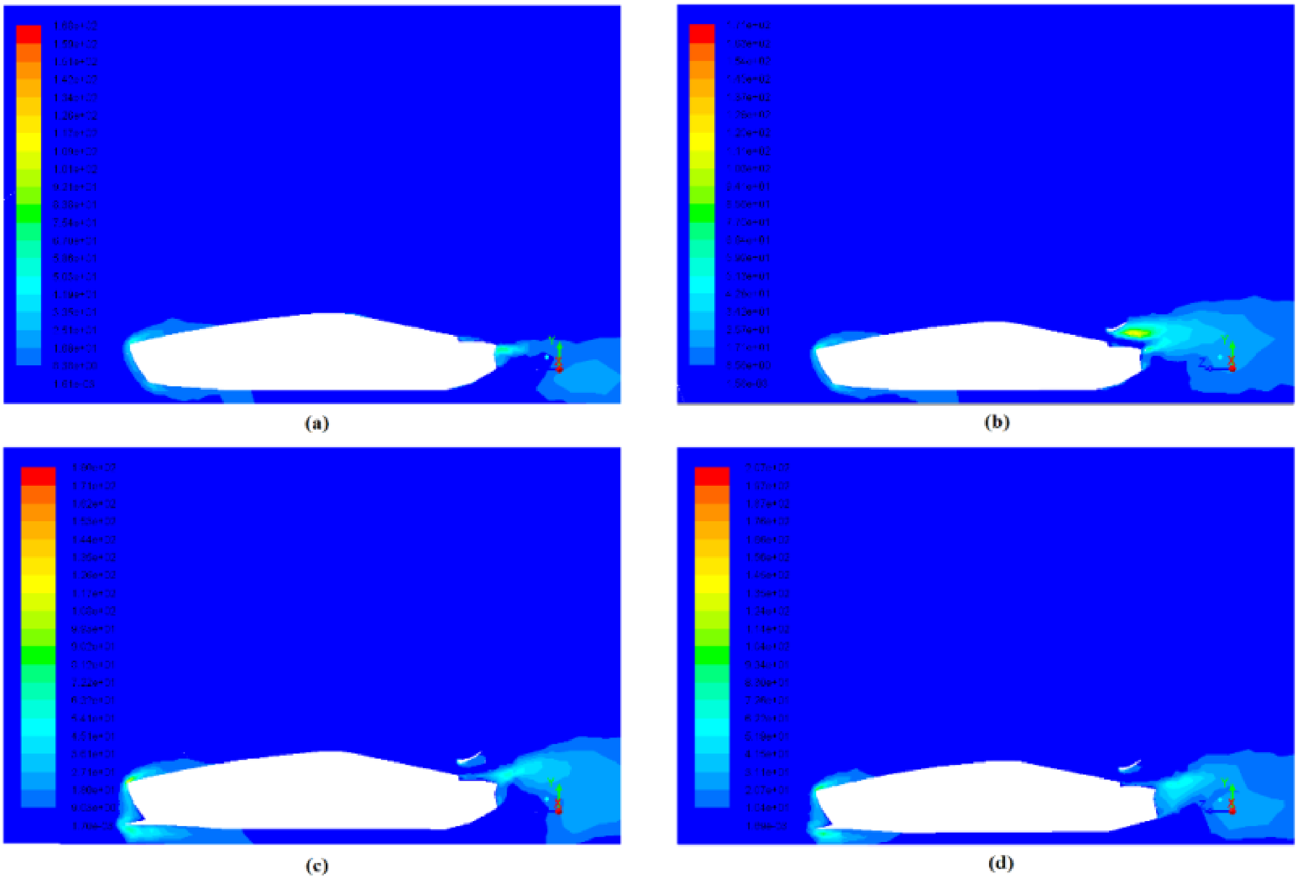

Figure 6. Turbulent kinetic energy contours of (a) CSC-1 (b) CSC-2 (c) CSC-3 and (d) CSC-4

3.2. 3D CFD analysis

The 3D analysis of half of the model vehicle, taking symmetry condition, is successful in predicting the drag, lift and flow characteristics like air flow and its velocity, vorticity magnitude, pressure coefficient and Reynolds number.

The aerodynamic performance characteristics, i.e. drag and lift, of the four configurations of the generic sports are tabulated in the Table 2.

The drag and lift performance of CSC-1, the basic design, is satisfactory considering the drag performance but in the case of lift, the performance should need improvement, as the lift coefficient is 0.386. It is observed that CSC-1 has the least drag coefficient of 0.364 of all the configurations of the car. In CSC-2 configuration, the aerodynamic performance is satisfactory considering the lift performance, as negative lift of -0.196 is obtained, but in the case of drag, it failed as the drag coefficient obtained is 0.517, which is more drag CSC-1. This increase in drag for CSC-2 is due to the generic design of the rear-end wing, which needs design optimisation, so as to obtain a better drag performance.

It is observed that, CSC-3 has a poor performance in terms of aerodynamic aspects because the drag has increased to 0.525 and the negative lift has decreased to -0.142.

Similar to CSC-2, CSC-3 also needs design optimisation for both front and rear-end wings.

The final configuration, CSC-4, has better performance when compared to both CSC-2 and CSC-3, but cannot achieve better drag as CSC-1.

The negative lift of CSC-4 is -0.291 and is very higher than CSC-2 and CSC-3 and even the drag obtained is 0.515, which is lower than that of obtained for both CSC-2 and CSC-3.

Therefore, unlike the front and rear-end wings, the rear-end diffuser does not need design optimisation and is good at performance. It can also be stated that, with a good design optimisation of front and rear-wing, the CSC-4 will perform even better than CSC-1 in terms of drag and will achieve a better aerodynamic performance.

All inferences drawn from the 2D analysis are mostly satisfied except for some modifications required in terms of drag reduction, downward force improvement and design optimisation.

ISSN 2457 – 5275 (Online, English)
ISSN 1842 – 4074 (Print, Online, Romanian)

Table 2.
Drag and Lift coefficients for all configurations of generic car

Generic car	Coefficient of Drag (C_d)	Coefficient of Lift (C_l)
CSC-1	0.363506	0.386403
CSC-2	0.517039	-0.196196
CSC-3	0.525174	-0.141638
CSC-4	0.514565	-0.291189

The velocity of air flowing around the surfaces of the vehicle body for all four configurations is shown in Figure 7 and it is also evident that the maximum velocity of air flow of both 2D and 3D analysis are identical and the trailing air flow for every configuration is clearly represented.
The CSC-1 has shown a good performance as per drag, which is least of all the configurations, but the lift is high and needs some body design modifications for better performance.
The trailing air flow of CSC-2 is almost similar to the 2D contour and clearly shows the flow of air behind the rear-end wing and also vortex at the rear-end. But yet the trailing air flow is in advantageous position, the design of the wing waned the aerodynamic performance of the vehicle.
Similar case is observed for CSC-3, as front-end wing just intensified the under body air flow, which eventually increased the pressure at bottom of the vehicle, leading to decrease in lift.
The design of front-end wing should be optimised according to the design of rear-end wing, which also needs design optimisation, so as to achieve better aerodynamic performance.
The final model CSC-4 really showed a better potential in aerodynamic performance when compared to CSC-2 and CSC-3, but needs the design modification for front and rear-end wings for improvement of drag reduction and achieving a drag lower than CSC-1. The velocity path-lines clearly show a better formation of primary trailing vortex, but cannot display the secondary trailing vortex clearly.
The pattern of trailing air flow at the rear-end is clear and non-intersecting, without any unnecessary vortices in the trailing air flow.

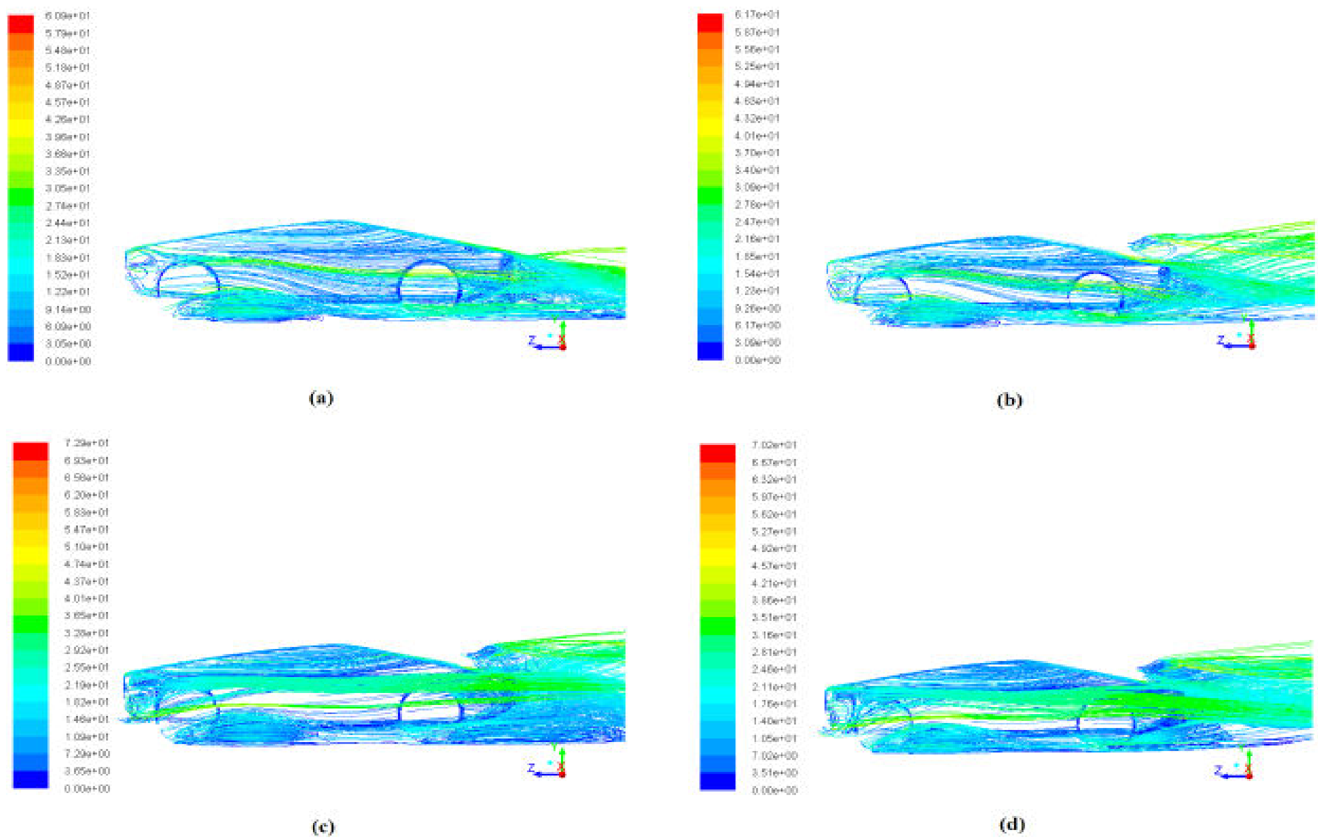

Figure 7. Velocity path-lines of air flow over the body of (a) CSC-1 (b) CSC-2 (c) CSC-3 and (d) CSC-4

The magnitude of vorticity is also analysed for each model and are shown in Figure 8.
The contour of vorticity magnitude for all configurations is limited to the highest magnitude predicted on the surface of the vehicle body, but the actual maximum vorticity magnitude obtained in the computational domain is way larger than the highest limitation applied for the contours.
The vorticity magnitude of CSC-1 is in the range of 0.003073045 - 13566.06 s^{-1} and limiting magnitude is the highest vorticity magnitude, 13566.06 s^{-1}.
The CSC-2 has a vorticity magnitude range of 0.001062883 - 80668.63 s^{-1} and CSC-3 has a vorticity magnitude range of 0.001388432 – 53509.01 s^{-1} and the vorticity magnitude range for CSC-4 is 0.0006576517 - 52380.1 s^{-1}. The limiting vorticity magnitude for CSC-2, CSC-3 and CSC-4 is 30000 s^{-1}.

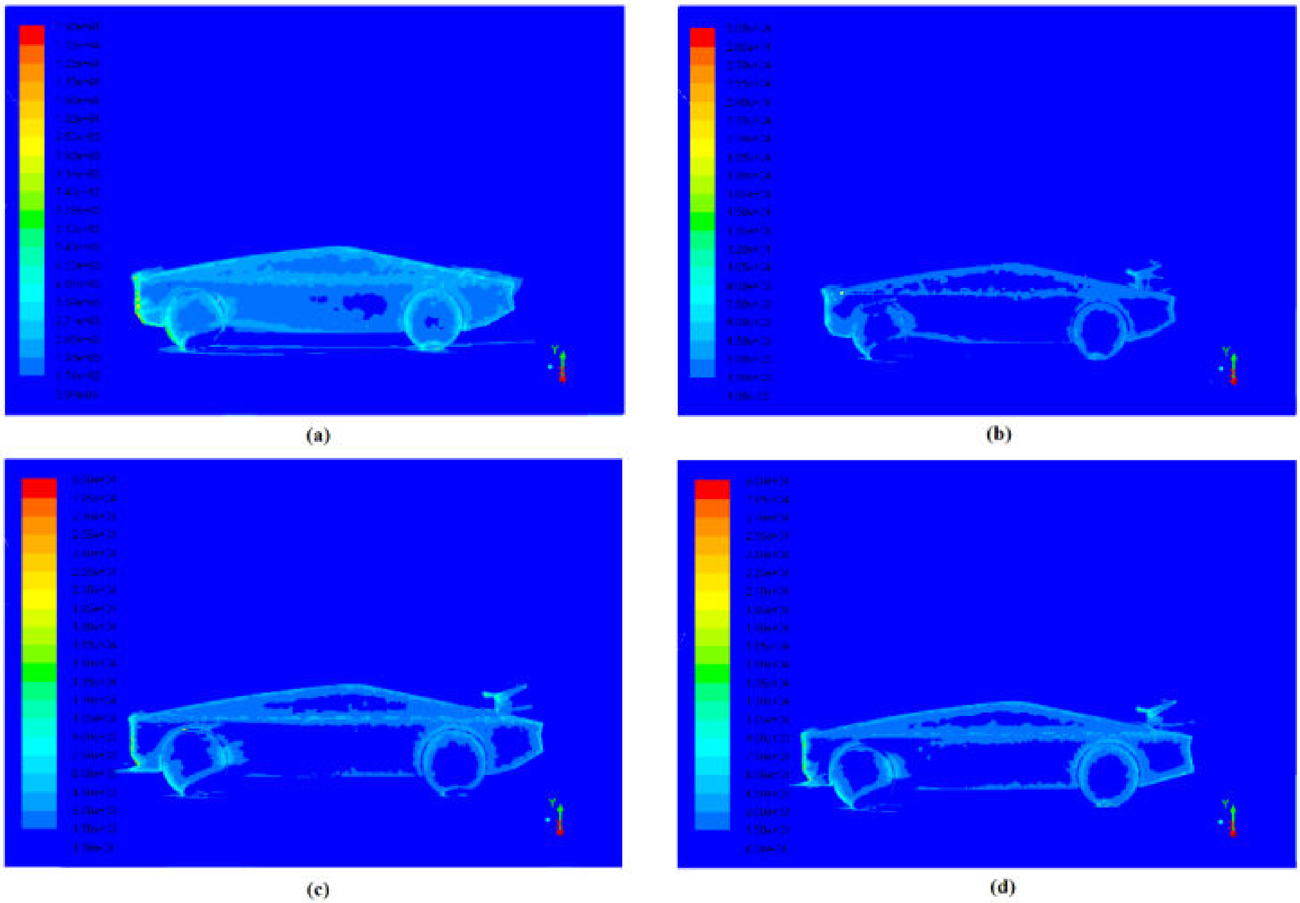

Figure 8. Contour of Vorticity magnitude of (a) CSC-1 (b) CSC-2 (c) CSC-3 and (d) CSC-4

The inferences from both 2D and 3D analysis, it is clear that the final configuration CSC-4 is best suitable for generic car model as it has shown a better aerodynamic performance in terms of drag, lift, trailing air flow, underbody air flow, vortices, velocity of air flow over the boundaries and surfaces when compared to CSC-2 and CSC-3, except that the drag is not lower than the basic model CSC-1. Therefore, a complete 3D analysis of the final configuration, CSC-4, is performed with computational domain larger than the previous one and the results showed the exact trailing air flow, containing the primary and secondary vortices created by streamlining and diffuser respectively, at the rear-end of the vehicle. The results of trailing air flow support the formation of secondary vortex from trailing air flow coming from under body of the vehicle due to the diffuser and the formation of primary vortices of the trailing flow is also observed.

4. CONCLUSION

The present investigation engrosses on studying the aerodynamic performance of a generic sports car, designed conceptually and to improve its aerodynamic performance by the application of various aerodynamic add-on devices.

ISSN 2457 – 5275 (Online, English)
ISSN 1842 – 4074 (Print, Online, Romanian)

The aerodynamic performance of the generic car is predicted through CFD simulation analysis and the simulation for both 2D boundary and 3D surfaces of the vehicle body of all configurations of generic car.
The preliminary results of 2D CFD analysis are helpful in understanding the velocity of air flow and turbulent kinetic energy dissipation over the surfaces of vehicle body.
The theory developed for understanding the aerodynamic performance clearly show that the performance of CSC-1 and CSC-4 will be better among all the models.
These 2D analysis inferences were supported by the results obtained from the 3D analysis, showing the lowest drag among the four configurations, of 0.363506 by CSC-1 and best negative lift performance by CSC-4 with lift coefficient of -0.291189.
It is observed that with the implementation of front and rear-end wings for CSC-2 and CSC-3, they have better negative lift than CSC-1 but the drag is very high when compared to CSC-1 and among them, CSC-3 has higher drag and lower negative lift than CSC-2, which implies that the design of front and rear-end wings need a design optimisation for better aerodynamic performance that CSC-1.
The CSC-4 is considered the best compared to CSC-2 and CSC-3 as the drag is lesser than the both and negative lift higher than the both but yet its drag is higher than CSC-1.
So it can be stated that with design optimisation of front and rear-end wings, the performance of CSC-4 will be higher than CSC-1.
The aerodynamic performance of CSC-1 is also very good but the lift developed is higher, for a sports car and obviously need aerodynamic add-ons for better lift performance.
The final results of the complete 3D analysis of CSC-4 gave support to the inferences from earlier 2D and 3D CFD simulations.
The primary vortices at the corners of rear-end side are very clearly visible in the figure and flow around the body surfaces is shown in Figure 9(a) and (b).
The higher drag reduction than CSC-2 and CSC-3 is due to the secondary vortex in the trailing air flow at the centre of rear-end, created by the flow of air through diffuser and is shown by Figure 9(c) and (d), in back and bottom view.
The results obtained from these CFD analysis are further used for reducing the drag and negative lift improvement to enhance the aerodynamic performance of CSC-4.

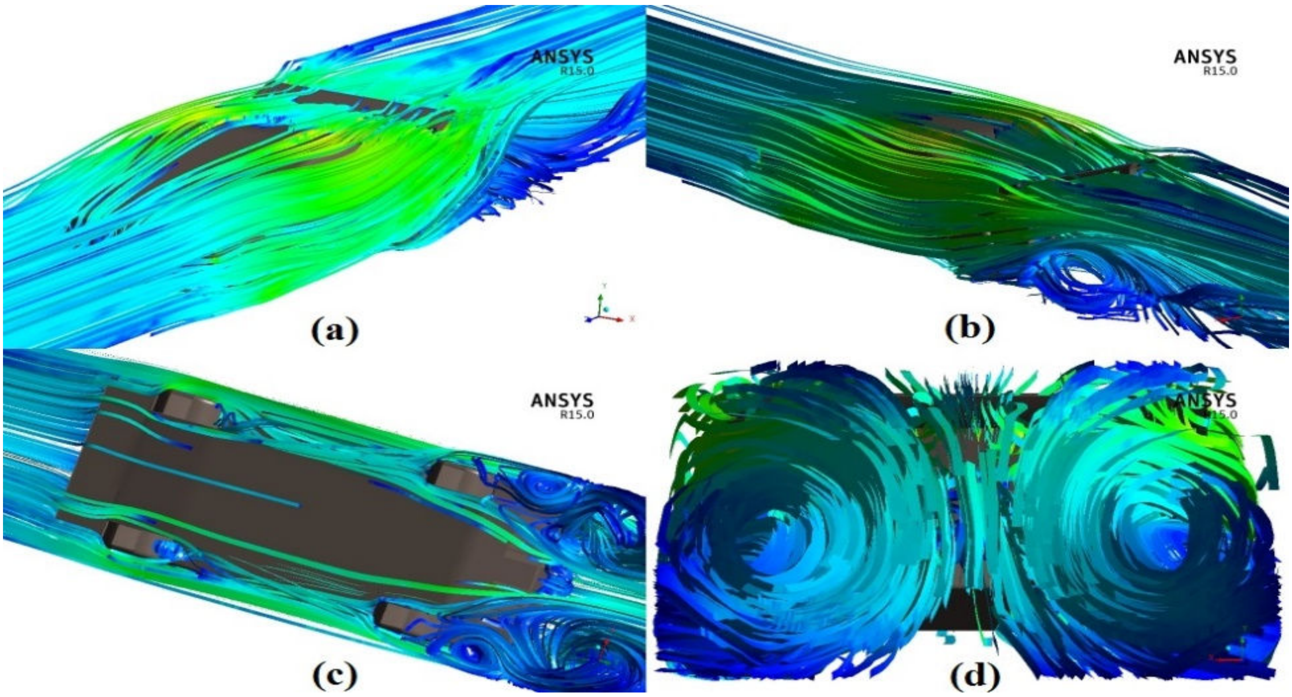

Figure 9. Air flow over complete CSC-4 model

REFERENCES

[1] Wolf-Heinrich Hucho., *Aerodynamics of Road Vehicle. English edition*, Butterworth-Heinemann Ltd, London, 1987.

[2] Katz J., *Race Car Aerodynamics – Designing for Speed. 2nd Edition*, Bentley Publishers, Massachusetts, 1995.
[3] Koike M., Nagayoshi T., Hamamoto N., *Research on aerodynamic drag reduction by vortex generators. Mitsubishi Motors*, Technical Reviews, No. 16, 2004.
[4] Versteeg H.K., Malalasekera W., *An Introduction to Computational Fluid Dynamics. Second Edition,* Pearson Eduction Limited, England, 2007.
[5] Andersson B., Andersson R., Hakansson L., Mortensen M., Sudiyo R., Wachem B.V., *Computational Fluid Dynamics for Engineers. First Edition,* Cambridge University Press, New York, 2012.
[6] Ahmed S.R., Ramm R., Faltin G., *Some salient features of the time averaged ground vehicle wake,* SAE Technical Paper, No. 840300, 1984.
[7] Han T., *Computational analysis of three-dimensional turbulent flow around a blu□ body in ground proximity*, AIAA Journal, Vol. 27, Issue 9, pag. 1213–1219, 1988.
[8] Han T., Hammond D.C., Sagi C.J., *Optimization of blu□ body for minimum drag in ground proximity*, AIAA Journal, Vol. 30, Issue 4, pag. 882–889, 1992.
[9] Gillieron P., Chometon F., *Modelling of stationary three dimensional separated flows around an Ahmed reference model*, ESAIM Proceedings. Vol. 7, pag. 173-182, 1999.
[10] Haoqin S., Xiaoxiang B., Jianhua L., Kai L., Mengxi C., *Jing S. Calculation and Analysis on Stealth and Aerodynamics Characteristics of a Medium Altitude Long Endurance UAV,* Procedia Engineering, Vol. 99, pag. 111-115, 2015.
[11] Pogni M., Petrone N., *Comparison of the aerodynamic performance of five racing bicycle wheels,* Procedia Engineering, Vol. 147, pag. 74 -80, 2016.
[12] Kontogiannis S.G., Ekaterinaris J.A., *Design, performance evaluation and optimization of a UAV*, Aerospace Science and Technology, Vol. 29, pag. 339-350, 2013.
[13] Asaia T., Honga S., Ijuin K., *Flow visualization of downhill ski racers using computational fluid dynamics*, Procedia Engineering, Vol. 147, pag. 44-49, 2016.
[14] Leusink D., Alfano D., Cinnella P., *Multi-fidelity optimization strategy for the industrial aerodynamic design of helicopter rotor blades*, Aerospace Science and Technology, Vol. 42, pag. 136-147, 2015.
[15] Chen G., Chen B., Li P., Bai P., Ji C., *Study of Aerodynamic Configuration Design and wind tunnel test for Solar powered Buoyancy-lifting Vehicle in the Near-space*, Procedia Engineering, Vol. 99, pag. 67-72, 2015.
[16] Guo W., Liu X., Yuan X., *Study on Natural Ventilation Design Optimization Based on CFD Simulation for Green Buildings*, Procedia Engineering, Vol. 121, pag. 573-581, 2015.
[17] Pottsa J. R., Masters D., *Validation of the Aerodynamic Loading on Basic Flying Disc Geometries derived from CFD Simulations*, Procedia Engineering, Vol. 112, pag. 400-405, 2015.
[18] Panagiotou P., Kaparos P., Salpingidou C., Yakinthos K., *Aerodynamic design of a MALE UAV*, Aerospace Science and Technology, Vol. 50, pag. 127-138, 2016.
[19] Blocken B., Toparlar Y., Andrianne T., *Aerodynamic benefit for a cyclist by a following motorcycle*, Journal of Wind Engineering & Industrial Aerodynamics, Vol. 155, pag. 1-10, 2016.
[20] Xia C., Shan X., Yang Z., *Wall interference effect on the aerodynamics of a high-speed train*, Procedia Engineering, Vol. 126, pag. 527-531, 2015.
[21] Li Y., Reimann B., Eggers T., *Numerical investigations on the aerodynamics of SHEFEX-III launcher*, Acta Astronautica, Vol. 97, pag. 99-108, 2014.
[22] Castelli M.R., Monte A.D., Quaresimin M., Benini E., *Numerical evaluation of aerodynamic and inertial contributions to Darrieus wind turbine blade deformation*, Renewable Energy, Vol. 51, pag. 101-112, 2013.
[23] Roncioni P., Rufolo G.C., Marini M., Borrelli S., *CFD rebuilding of USV-DTFT1 vehicle in-flight experiment*, Acta Astronautica, Vol. 66, pag. 1201-1219, 2010.
[24] Dhaubhadel M.N., *Review: CFD Applications in the Automotive Industry*, Journal of Fluids Engineering, Vol. 118, pag. 647-653, 1996.
[25] Newbon J.J., Dominy R.G., Sims-Williams D.B., *Investigation into the effect of the wake from a generic formula one car on a downstream vehicle*, International vehicle aerodynamics conference, 2014.
[26] Hassan S.M.R., Islam T., Ali M., Islam Q., *Numerical Study on Aerodynamic Drag Reduction of Racing Cars*, Procedia Engineering, Vol. 90, pag. 308-313, 2014.

ISSN 2457 – 5275 (Online, English)
ISSN 1842 – 4074 (Print, Online, Romanian)

[27] Piechna J., Rudniak L., Piechna A., *CFD Analysis of the Central Engine Generic Sports Car Aerodynamics*, 4th European Automotive Simulation Conference, 2009.
[28] Watkins S., Vino G., *The effect of vehicle spacing on the aerodynamics of a representative car shape*, Journal of Wind Engineering and Industrial Aerodynamics, Vol. 96, pag. 1232-1239, 2008.
[29] Zhang X., Toet W., Zerihan J., *Ground effect aerodynamics of race cars*, Applied Mechanics Reviews, Vol. 59, pag. 33-49, 2006.
[30] Lewis R., Cross M., Ludlow D., *The influence of rotating wheels on the external aerodynamic performance of a vehicle*, International vehicle aerodynamics conference, 2014.
[31] Gnech A., *Development of a Robust Workflow for a CFD Analysis of External Aerodynamics in a Virtual Wind Tunnel*, RWTH Aachen University, 2012.
[32] Damjanovic D., Kozak D., Zivic M., Ivandic Z., Baskaric T., *CFD analysis of concept car in order to improve aerodynamics*, International Scientific and Expert Conference, 2010.
[33] Buljac A., Dzijan I., Korade I., Krizmanic S., Kozmar H., *Automobile aerodynamics influenced by airfoil-shaped rear wing*, International Journal of Automotive Technology, Vol. 17, Issue 3, pag. 377-385, 2016.
[34] Uddi M., Mohrfeld-Halterman J.A., *Quasi steady-state aerodynamic model development for race vehicle simulations*, Vehicle System Dynamics, Vol. 54, Issue 1, pag. 124-136, 2016.
[35] Jugulkar L.M., Singh S., Sawant S.M., *Fluid flow modeling and experimental investigation on automobile damper*, Construction and Building Materials, Vol. 121, pag. 760-772, 2016.
[36] Dobronsky S., *Aerodynamic Improvement of the BYU Supermileage Vehicle*, Brigham Young University, 2015.
[37] Meederira P.B., *Aerodynamic development of a IUPUI Formula SAE specification car with Computational Fluid Dynamics (CFD) analysis*, IUPUI School of Engineering and Technology, 2015.
[38] Sesta V.O.D., *Modelling and aerodynamic simulation of a vehicle and failure analysis of a laminated front fender*, Instituto Superior De Engenharia De Lisboa, 2014.
[39] Khalighi B., Jindal S., Iaccarino G., *Aerodynamic flow around a sport utility vehicle-computational and experimental investigation*, Journal of Wind Engineering and Industrial Aerodynamics, Vol. 107–108, pag. 140–148, 2012.
[40] Canada E., *Aerodynamic analysis and optimisation of the rear wing of a WRC car*, Oxford Brookes University, 2012.
[41] Nasir R.E.M., Mohamad F., Kasiran R., Adenan M.S., Mohamed M.F., Mat M.H., Ghani A.R.A., *Aerodynamics of ARTeC's PEC 2011 EMo-C Car*, Procedia Engineering, Vol. 41, pag. 1775-1780, 2012.
[42] Wojciak J. D., *Quantitative analysis of vehicle aerodynamics during crosswind gusts*, Technische Universität München, 2012.
[43] User's Guide, ANSYS FLUENT 12 Documentation.
[44] Immersed Boundary Module Manual, ANSYS FLUENT 12 Documentation.
[45] ANSYS Fluent Tutorial Guide, Release 15.0 Documentation.

ISSN 2457 – 5275 (Online, English)
ISSN 1842 – 4074 (Print, Online, Romanian)

ASPECTS REGARDING THE ANALYSIS AND RECONSTRUCTION OF CAR CRASHES

Ramona – Monica STOICA [*], Virgilius – Justinian RĂDULESCU, Daniel NEAGU, Cătălin TROCAN, Ion COPAE

Military Technical Academy, Bulevardul George Coşbuc, Nr. 39-49, 050141, Bucharest, Romania

(Received 17 July 2017; Revised 02 August 2017; Accepted 09 August 2017)

Abstract: *The paper highlights that the process of analysis and reconstruction of car crashes is defined by great complexity and by the existance of multiple parametric, functional and running uncertainties. This complexity is due to some difficulty regarding mathematical description of showing, as real as possible, the automotive impact phenomenon, and automotive kinematics and dynamics. The complexity of analysis and reconstruction increases when driving comes along with side-slip, unequal braking forces, pitching movement, objects dismission, wheels locking, tires burst or it is influenced by multiple collisions with fixed obstacles or with other vehicles. In the paper there are presented and applied concepts and algorithms used in the analysis and reconstruction of car crashes, which belong to technical mechanics, systems theory, uncertainty theory, intervals analysis, automotives mechanics, signal theory. Likewise, there are analysed main mathematical models that are currently used for the analysis and reconstruction of car crashes. Within the paper there are presented examples of reconstruction for car crashes occurred on public road.*

Key-Words: *Car crashes, reconstruction, collisions.*

1. INTRODUCTION

The advance in the number of vehicles and the infrastructure development have led to an increased traffic and number of car crashes. The process of analysis and car crash reconstruction is defined by great complexity and by the existence of multiple parametric, functional and running uncertainties. This complexity is due to some difficulties, including of mathematical description, in describing as real as possible, the vehicle kinematics and dynamics.

All existing difficulties, currently there are analytical mathematical models which can describe a car crash, as well as multiple specialty literature.

Specialized software simulations and tests conducted in various research institutes, universities and laboratories of the construction companies assure a wide database of actual information obtained during accidents or car crash simulation.

2. UNCERTAINTIES IN CAR CRASH RECONSTRUCTION

Experts frequently use uncertainties, mostly because there are encountered not only in technical field but in other domains too. To provide some practical examples of road accidents, there are uncertainties regarding weight of moving vehicles, mass moments of inertia, adhesion coefficient, the position of centre of gravity, the position of centre of impact, restitution coefficient, tangential friction coefficient between vehicles, observation-reaction time and driver action etc.

As it can be seen, uncertainties are related to those three factors participant to the car crash: the vehicle, the runway and the driver.

In general, from a quantitative point of view, uncertainties can be defined as an expected set of values.

[*] *Corresponding author e-mail:* monik_dep@yahoo.com

ISSN 2457 – 5275 (Online, English)
ISSN 1842 – 4074 (Print, Online, Romanian)

For example, values of some functional, constructional and operational parameters can be estimated: vehicle weight depending on number of passengers, the luggage and quantity of fuel; adhesion coefficient for a certain road category and depending on the runway status, tyre pressure and wear etc. Follow-up is an example of uncertainty that occurs in analysis and reconstruction of car crashes.
As it is known, the adhesion coefficient on a worn dry asphalt runway has values in the interval $\varphi = [0.6; 0.8]$ if the speed is lower than 48 km/h and $\varphi = [0.55; 0.7]$ if the speed is higher than 48 km/h [1].
In the first case it can be written:

$$\varphi = 0.7 \pm 0.1 = 0.7\left(1 \pm \frac{0.1}{0.7}\right) = 0.7\left(1 \pm 0.1429\right) = 0.7\left(1 \pm \frac{14.29}{100}\right) \tag{1}$$

Therefore, from the information given in specialty literature, it can be concluded that in case of driving on a worn dry asphalt runway, with a speed lower than 48 km/h, the value of adhesion coefficient can be adopted 0.7 with an uncertainty of 14.29%.
It should be noted that the values presented in specialty literature are all obtained based on previous measurements. In the case presented above, if there were performed experiments with a car, the real value of adhesion coefficient is not precisely known and that is why an average value from specialty literature is adopted (0.7 in the example from above).
If no other information are available, it would be accurate to perform calculations with the full range of recommended values because the adhesion coefficient represents an uncertain variable; obviously, the result obtained would not be a unique value, but an interval of values.
Another example targets uncertainties related to driver reaction time and the driver-vehicle assembly reaction time.
Reaction time, a term frequently used in native literature or perception-reaction time, which is a concept frequently used in occidental specialty literature, is considered one of the key elements in establishing opportunities for crash avoidance, mandatory requirement imposed by judicial agencies.
Thus, in specialty literature, to determine vehicle brake space in order to avoid an accident, for example, hitting a pedestrian, it is used the ratio:

$$S_o = \left(t_1 + t_2 + 0{,}5 t_3\right)\frac{V_a}{3.6} + \frac{V_a^2}{2 \cdot 3.6^2 g\varphi} \tag{2}$$

in which we note:
V_a – vehicle speed, in km/h;
g – gravitational acceleration, g=9.81 m/s^2;
φ – adhesion coefficient;
t_1 – driver reaction time, for which our specialty literature indicates values in the range:

$$t_1 = \left[0.5; 1.0\right] \text{s} \tag{3}$$

t_2 – time between the moment when the brake pedal is actuated by the driver and when the actual braking action starts, for which the specialty literature indicates values in the range:

$$t_2 = \left[0.2; 0.5\right] \text{s} \tag{4}$$

t_3 - time between the begining of braking force and its maximum value, for which the specialty literature indicates, in case of hydraulic brakes, to adopt the following value:

$$t_3 = 0.1 \text{ s} \tag{5}$$

Other aspects will be presented regarding driver reaction time t_1.

 ISSN 2457 – 5275 (Online, English)
ISSN 1842 – 4074 (Print, Online, Romanian)

Therefore, in specialty literature there are presented factors with influence on driver reaction time [2], with quantitative assessment on it; some of these influences effects values from the interval (3):
- in case of reduced visibility, response time must be increased by 25-50%:

$$t_1 = [0.5; 1.0] \cdot (1 + [0.25; 0.50]) = [0.62; 1.50]\ \mathrm{s} \tag{6}$$

- fatigue; for example, at the end of a working day, the reaction time increases by 40-60%:

$$t_1 = [0.5; 1.0] \cdot (1 + [0.4; 0.6]) = [0.7; 1.6]\ \mathrm{s} \tag{7}$$

- on slippery roads, the reaction time must be increased by 15-20%:

$$t_1 = [0.5; 1.0] \cdot (1 + [0.15; 0.20]) = [0.57; 1.20]\ \mathrm{s} \tag{8}$$

- age; for example, in case of drivers over 45 years old, reaction time increases by 40-60% as opposed to the reaction of drivers below 30 years old:

$$t_1 = [0.5; 1.0] \cdot (1 + [0.4; 0.6]) = [0.7; 1.6]\ \mathrm{s} \tag{9}$$

- traffic intensity; if traffic is congested, reaction time must be increased by 1 s:

$$t_1 = [0.5; 1.0] + 1 = [1.5; 2.0]\ \mathrm{s} \tag{10}$$

- when the mobile phone is used, reaction time increases by 0.5 s:

$$t_1 = [0.5; 1.0] + 0.5 = [1.0; 1.5]\ \mathrm{s} \tag{11}$$

- alcohol consumption; for example, a blood level of 0.3-0.5 g^{o}/oo determines an increase of time reaction by 25%:

$$t_1 = [0.5; 1.0] \cdot (1 + 0.25) = [0.62; 1.25]\ \mathrm{s} \tag{12}$$

As it can be seen from these ratios, it is necessary to perform operations with ranges of values, meaning to use interval analysis.
Also, it is observed that some of the increase in reaction time cannot be imputed to the driver (low visibility, age etc.), but others may be (phone use, blood alcohol level).
To highlight those presented above regarding the importance of reaction time when we analyse possibilities of car crash avoidance, it is considered a case in which a 48 years old individual is driving a car during night.
Accordingly to those presented, driver reaction time which is given by formula (3) must be increased by values given in expressions (6), (7) and (9):

$$t_1 = [0.5; 1.0] \cdot (1 + [0.25; 0.50] + [0.4; 0.6] + [0.4; 0.6]) = [1.02; 2.70]\ \mathrm{s} \tag{13}$$

Follow-up it is considered the example in which the driver must avoid hitting a pedestrian that he observes from a distance of 24 m, the vehicle is driving on a polished asphalt road, where the adhesion coefficient is in the range:

$$\varphi = [0.55; 0.75] \tag{14}$$

the driving is in the city, the speed is considered V_a<48 km/h.

ISSN 2457 – 5275 (Online, English)
ISSN 1842 – 4074 (Print, Online, Romanian)

From formula (2) results the speed that the vehicle should have in order for the driver to avoid hitting a pedestrian that he observed from a distance of S_o=24 m (only positive values of speed are accepted):

$$V_a = -35.32\varphi(t_1+t_2) - 17.66\varphi t_3 + 13.89\sqrt{1.32\varphi S_o + \left[2.54\varphi(t_1+t_2)+1.27\varphi t_3\right]^2} \quad (15)$$

If we replace all known values of parameters, t_1 from expression (13), with t_2 from expression (4), with t_3 from expression (5) and with φ from expression (14), from ratio (15) results the interval of values for vehicle speed:

$$V_a = [23.4; 38.3] \text{ km/h} \quad (16)$$

Therefore, it can be estimated that the driver avoids the accident, in those circumstances, if vehicle speed is lower than 23.4 km/h.
If you do not take into account the uncertainties due to the driver (age, poor visibility, fatigue), then t_1 is adopted in relation (3), and as a result of the expression (15) results:

$$V_a = [38.1; 45.2] \text{ km/h} \quad (17)$$

According to this interval, results that, for example, the driver could avoid the accident if the car speed is 30 km/h (lower than 38.1 km/h), which is not true because in a real situation this value must be lower than 23.4 km/h, as it resulted from expression (16).

3. CAR CRASH RECONSTRUCTION IN CASE OF UNCERTAINTIES

From those presented above results that in order to consider the actual conditions in which an accident took place, uncertainties related to the specific case that was analyzed must be taken into account; this involves operation with interval of values and not with single value [3].
For that matter, the mere fact that specialty literature present value ranges of sizes (eg of adhesion coefficient) denotes the existence of uncertainties on them.
As an example it is considered a rear centre collision like in figure 1 between vehicles A1 and A2, of known mass m_1=1690 kg and m_2=1580 kg. It is also known that A1 vehicle has covered a distance after the collision of S1 = 23.97 m and A2 vehicle a distance of S2 = 25.83 m, both along the line of the centers of gravity CG_1 and CG_2.

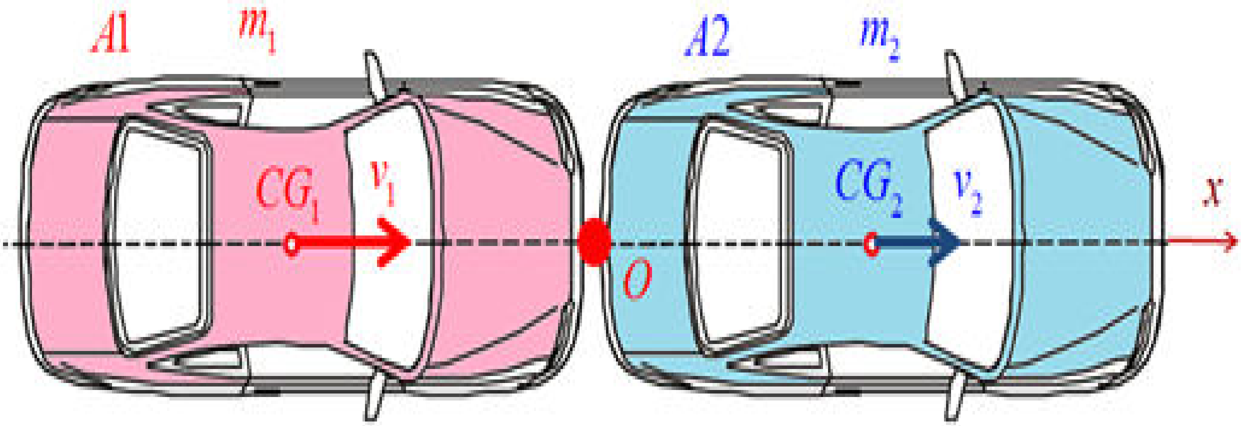

Figure 1. Rear centre collision between two vehicles

It is targeted the influence of restitution coefficient on collision sizes, when the adhesion coefficient is considered $\varphi = 0.65$.

ISSN 2457 – 5275 (Online, English)
ISSN 1842 – 4074 (Print, Online, Romanian)

Considering the distances traveled by the vehicles after collision and the fact that their deceleration is constant after the impact and until the actual stop, the separation speeds V_1 and V_2 can be established:

$$V_1 = 3.6\sqrt{2g\varphi S_1};\ V_2 = 3.6\sqrt{2g\varphi S_2} \tag{18}$$

from where results V_1=62.9 km/h and V_2=65.3 km/h, values shown in figure 2a.
To establish the influence of restitution coefficient e, it is varied between the most common values encountered in practice e=[0.1; 0.3]. In order to establish impact speeds v_1 and v_2 of the two vehicles, it is used the mathematical description in case of centre collisions [4]:

$$\begin{bmatrix} m_1 & m_2 \\ e & -e \end{bmatrix} \cdot \begin{bmatrix} v_1 \\ v_2 \end{bmatrix} = \begin{bmatrix} m_1 & m_2 \\ -1 & 1 \end{bmatrix} \cdot \begin{bmatrix} V_1 \\ V_2 \end{bmatrix} \tag{19}$$

or in a limited form:

$$\mathbf{A} \cdot \mathbf{x} = \mathbf{B} \cdot \mathbf{x}_0 \tag{20}$$

where we note:

$$\mathbf{A} = \begin{bmatrix} m_1 & m_2 \\ e & -e \end{bmatrix}; \mathbf{B} = \begin{bmatrix} m_1 & m_2 \\ -1 & 1 \end{bmatrix}; \mathbf{x} = \begin{bmatrix} v_1 \\ v_2 \end{bmatrix}; \mathbf{x}_0 = \begin{bmatrix} V_1 \\ V_2 \end{bmatrix} \tag{21}$$

with **x** the vector of the unknown v_1 and v_2, meaning the solution:

$$\mathbf{x} = \mathbf{A}^{-1} \cdot \mathbf{B} \cdot \mathbf{x}_0 \tag{22}$$

If we vary e in the system (19) results the values of impact speeds from figure 2a.

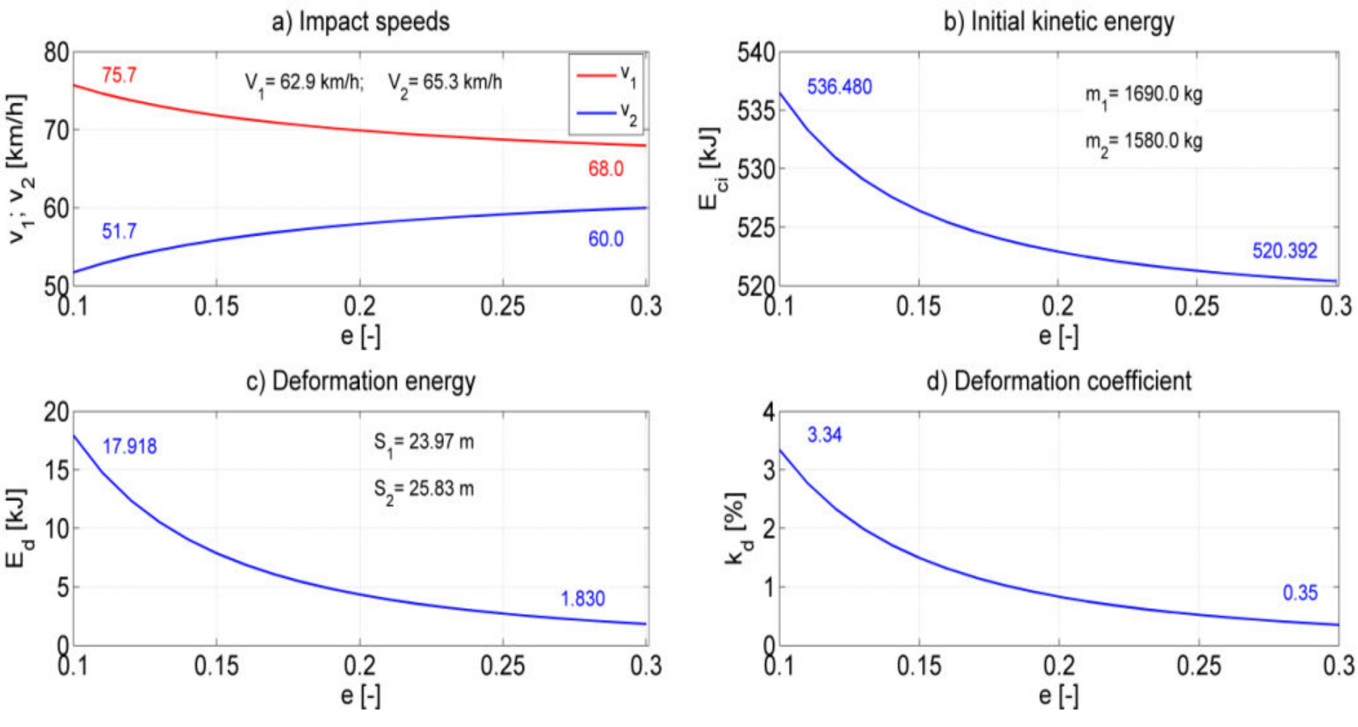

Figure 2. The influence of restitution coefficient on impact sizes between two vehicles, rear centre collision

ISSN 2457 – 5275 (Online, English)
ISSN 1842 – 4074 (Print, Online, Romanian)

As it can be seen from figure 2a, the size of restitution coefficient has the efect of decrease for the impact speed v_1 of A1 vehicle and the increase of impact speed v_2 of A2 vehicle, in the graph are also being shown the associated extreme values.
Likewise, from figure 2a it can also be observed that after the impact, the speed of A1 vehicle decreased, and the speed of A2 vehicle increased.
Finally, from figure 2a it can also be observed that impact speeds of A1vehicle are higher than the one of A2 vehicle ($v_1>v_2$), which is accurate physical speaking, A1vehicle hitting the rear of A2 vehicle (figure 1).
From figure 2b it is observed that the kinetic energy from the begining of impact is decreasing once the restitution coefficient is increasing.
The graph from figure 2c shows that deformation energy decreases with the increase of restitution coefficient. From figure 2d there can also be observed the existence of smaller values of deformation coefficient (k_d=0.35-3.34%), explained by the fact that there is a rear collision and not a head-on collision. Therefore, there are obtained ranges of values for the impact sizes in case of uncertainties regarding the restitution coefficient.
If we also consider uncertainties regarding the adhesion coefficient (considered to be constant), then there are obtained three-dimensional graphs of variation in case of impact sizes.
In this regard, follow-up it is considered an example of a light crash, without pitching moment, where the angular velocities from before the impact and after are small; therefore there can be neglected the yaw movements, rolling movements and pitching movement.
Based on these assumptions results that the impact can be mathematically described just by using the principle of conservation of momentum.
Aplying this principle on the two axes from plane [4], results the mathematical description of the car crash (index 1 for A1 vehicle, index 2 for A2 vehicle):

$$\begin{cases} m_1 v_1 \cos\theta_1 + m_2 v_2 \cos\theta_2 = m_1 V_1 \cos\Theta_1 + m_2 V_2 \cos\Theta_2 \\ m_1 v_1 \sin\theta_1 + m_2 v_2 \sin\theta_2 = m_1 V_1 \sin\Theta_1 + m_2 V_2 \sin\Theta_2 \end{cases} \tag{23}$$

in which m_1=1700 kg and m_2=1600 kg represents the mass of the two vehicles.
From the car crash scene there are known the distances covered by vehicles after the impact S_1=23.26 m and S_2=24.7 m, as well as the angles of direction for the separation speeds: Q_1=42 degrees and Q_2=75 degrees.
In addition, for the adhesion coefficient φ it is adopted the average value: $\varphi_1 = \varphi_2 = 0.65$.
In this case is studied the influence of angles of direction for impact speeds q_1 and q_2 on sizes that define the collision.
So, angles of direction for impact speeds are adopted as uncertain variables: q_1=74-78 degrees and q_2=10-14 degrees; so, it is considered that there are uncertainties regarding angles of direction for impact speeds.
If it is considered that between impact position and stop positions the deceleration remains constant, separation speeds are obtained from formulas [4]:

$$V_1 = 3.6\sqrt{2\varphi_1 g S_1} = 62 \text{ km/h}; \; V_2 = 3.6\sqrt{2\varphi_2 g S_2} = 63.9 \text{ km/h} \tag{24}$$

Based on those presented results that in the algebraic system (23) the impact speeds v_1 and v_2 are unknown, and all the other sizes are known as unique values, or as interval of values.
By resolving this algebraic system with intervals, there are obtained the values of impact speeds from figure 3 in spatial/tridimensional representation, where there is also presented an example (point A from the two graphs).
Graphs from figure 3 show that once the angles of direction for the impact speeds increases, impact speed v_1 decreases and impact speed v_2 increases.
Impact speeds have values in the ranges $v_1 = [97.2; 90.9]$ km/h and $v_2 = [37.6; 46.8]$ km/h , the variation type from the interval is according to the increase of the two angles, q_1 and q_2.

ISSN 2457 – 5275 (Online, English)
ISSN 1842 – 4074 (Print, Online, Romanian)

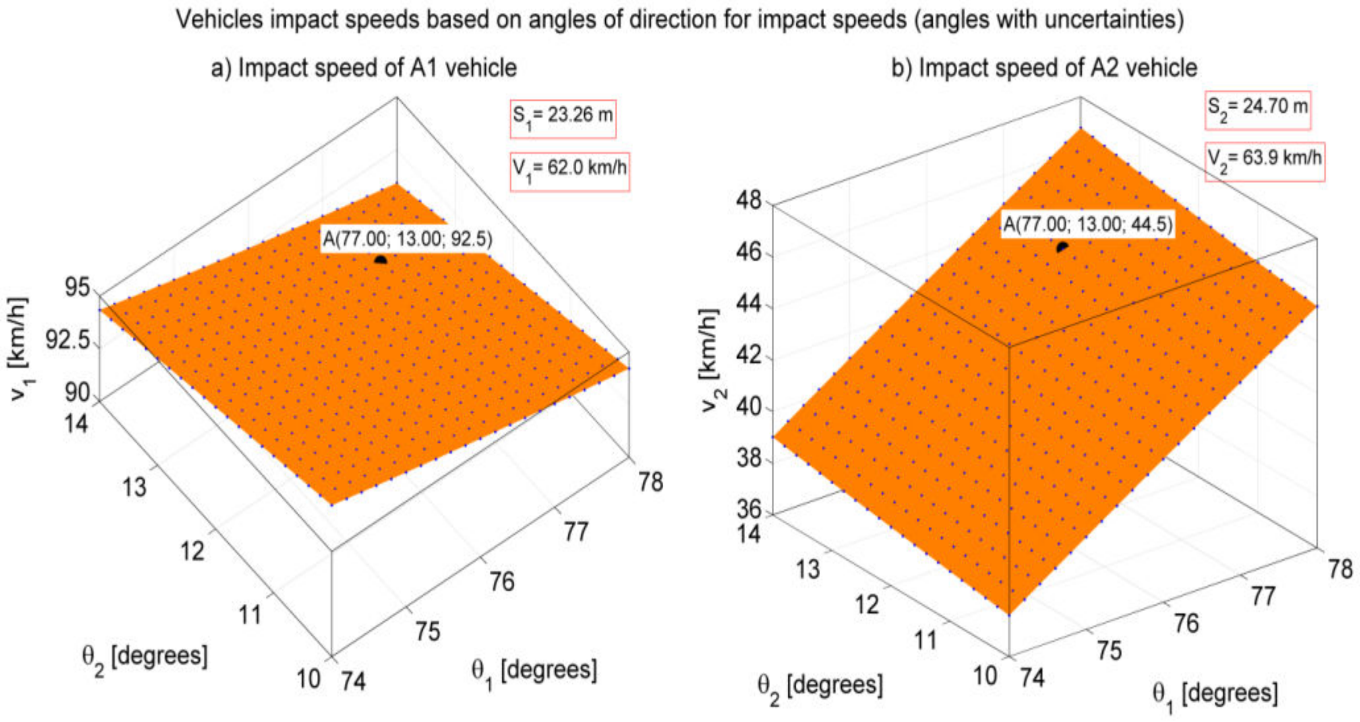

Figure 3. Vehicles impact speeds based on angles of direction for impact speeds (angles with uncertainties)

4. CONCLUSIONS

A more realistic car crash reconstruction must take into account different uncertainties, that is why the associated sizes must be given as interval of values.
This involves the use of interval analysis and uncertainty theory.

This work was presented at the International Congress of Automotive and Transport Engineering CONAT 2016, Brasov, Romania and it was published in Proceedings of the Congress (ISSN 2069-0401).

REFERENCES

[1] Nivedita Bisht, Sapna Singh : *Analytical study of different network topologies*: International Research Journal of Engineering and Technology : Volume: 02 Issue: 01 :Mar 2015;
[2] Nazmus Saquib, Md. Sabbir Rahman Sakib : ViSim: *A user-friendly graphical simulation tool for performance analysis of MANET routing protocols* : Mathematical and Computer Modelling 53 (2011) 2204–2218;
[3] Sachin Kumar Gupta, R. K. Saket : *Performance metric comparison of aodv and dsdv routing protocols in manets using ns-2*: International Journal of Research and Reviews in Applied Sciences : Volume 7, June 2011;
[4] Spinder Kaur, Harpreet Kaur : *Implementing RSA Algorithm in MANET and Comparison with RSA Digital Signature* : INTERNATIONAL JOURNAL FOR ADVANCE RESEARCH IN ENGINEERING AND TECHNOLOGY : Volume 3, Issue V, May 2015;
[5] C. Sreedhar, Dr. S. Madhusudhana Verma, Prof. N. Kasiviswanath : *A Survey on Security Issues in Wireless Ad hoc Network Routing Protocols* : International Journal on Computer Science and Engineering: Vol. 02, No. 02, 2010;
[6] Davide Benetti, Massimo Merro, Luca Vigan : Model Checking Ad Hoc Network Routing Protocols: ARAN vs. endair A: Software Engineering and Formal Methods (SEFM), 2010 8th IEEE International Conference;
[7] Intelligent Transportation Systems, Joint Program Office, *Intelligent transportation systems (ITS) Information Security Analysis*, U.S. Highway Administration, Department of Transportation, Federal Highway Administration, 1997.

ISSN 2457 – 5275 (Online, English)
ISSN 1842 – 4074 (Print, Online, Romanian)

[8] Bryan Parno, Adrian Perrig,: *Challenges in Securing Vehicular Networks*: http://www.sparrow.ece.cmu.edu.

[9] Maxim Raya, Panos Papadimitratos :*Securing Vehicular Communications*: http://www.ece.cmu.edu.

ISSN 2457 – 5275 (Online, English)
ISSN 1842 – 4074 (Print, Online, Romanian)

STUDIES ABOUT THE FRONT BUMPER PERFORMANCE DURING A PEDESTRIAN LEG IMPACT

Bogdan-Alexandru CONSTANTIN*, Daniel IOZSA, Gheorghe FRĂŢILĂ

Politehnica University of Bucharest, Splaiul Independentei, Nr. 313, Bucharest, Romania

(Received 17 July 2017; Revised 07August 2017; Accepted 17 August 2017)

Abstract: *A continuous evolution of requirements and standards sheds over the development of new vehicles (for example : EuroNCAP ratings) in order to create competition between same market models customer related. The pedestrian impact protection has to be permanently improved as the damage of the front end structure of the vehicle to be reduced to minimal. The European Community has had impressive success in achieving the highest pedestrian protection level on the globe. In 2013, 5.712 pedestrians were killed in road accidents in the EU, which in 22%of the fatalities. In the last decade, in the European Union, pedestrian fatalities were reduced by 37%, while the total number of fatalities was reduced by almost 45%. The front end structure, including the bumper, responds for the absorption of the kinetic energy created during the impact with maximum efficiency in order to avoid the large deformation of structural components and good behavior during a pedestrian impact. This is only one of the constraints that the front end structure has to cope with, additionally we can mention the dimensioning of the front end of the vehicle which can affect the packaging, which is mainly influenced by the design, styling and the pedestrian requirements intended to be accomplished by the vehicle. The present paper focuses on the pedestrian impact, offering an overview over the actual state, the load configuration, the applicable regulation, the challenging requirements of a modern front structure, which the modern bumper has to comply with and the finite elementsimulation of this kind of test.*

Key-Words: *Pedestrian impact, finite element, analysis simulation, EuroNCAP.*

1. INTRODUCTION

Recently, based on the help of advanced development of software and hardware equipment for numerical simulation, the period of time in which a project is finished and a new car is launched on the market has become smaller and smaller.

The competition on the automobile market has lead constructors to seek, apply and improve the latest techniques in the car manufacturing. The numerical simulation has gained more and more terrain facing the need of cost efficiency and rapidity of the project development.

After the manufacturing, a car has to pass in the first place the requirements of the homologation agencies and secondly, the very popular ranking tests (EuroNCAP).

Potential problems, which can affect the quality of the product over its life are identified and removed during the project phase. Using virtual prototyping and numerical simulation, we can improve the performance and the cost of the part before is it actually built. In addition to the numerical test, a physical one is carried out in addition to the numerical one in order to validate that the part meets the requirements. As a consequence, the need to build several sets of physical prototypes of the parts has decreased to a very small number, thus saving time and money.

The advantage of numerical simulation over the physical test consists in observing immediately if one part of the assembly does not comply with the specifications, rather than following an expensive testing procedure and waiting between the test and the post-processing of the results.

Thus, we can define the needed adjustments and rerun the simulation until we obtain the desired results. More precisely, while waiting several days for the physical test results for one crash configuration, we can numerically test hundreds of parameters simultaneously while observing in real time the global effects. If it shows that with the current front bumper design it is impossible to attain the required performances, a geometry change can be proposed.

* *Corresponding author e-mail:* constantin.bogdan.alexandru@gmail.com

ISSN 2457 – 5275 (Online, English)
ISSN 1842 – 4074 (Print, Online, Romanian)

2. TRAFFIC SAFETY FACTS

The European Community has had impressive success in achieving the highest pedestrian protection level on the globe. In 2013, 5.712 pedestrians were killed in road accidents in the EU, which is 22% of all fatalities. In the last decade, in the European Union, pedestrian fatalities were reduced by 37%, while the total number of fatalities was reduced by almost 45%.
Below in figure 1, please see the evolution of the pedestrian causalities between 2004 and 2013 in European Union.
The rate of pedestrian deaths in European Union countries varies from 3 pedestrian fatalities per million population in the Netherlands to more than 35 pedestrian fatalities per million population in Romania, a rate about 12 times higher.

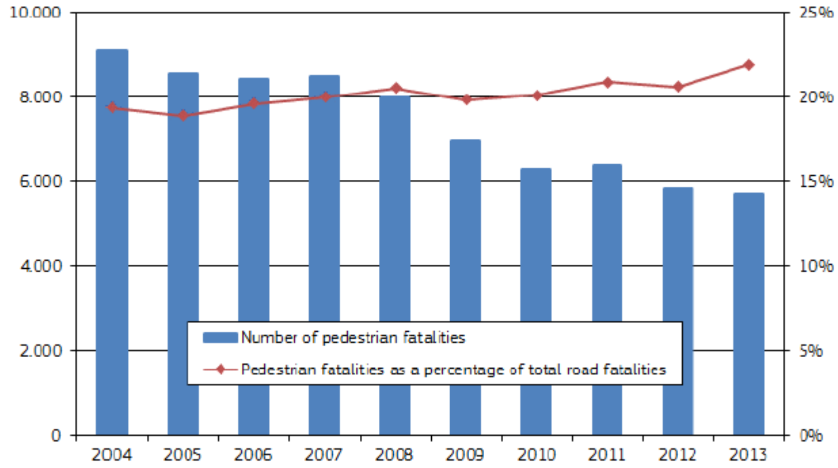

Figure 1. Number of pedestrian fatalities and percentage of all road fatalities in European Union, 2004-2013 [5]

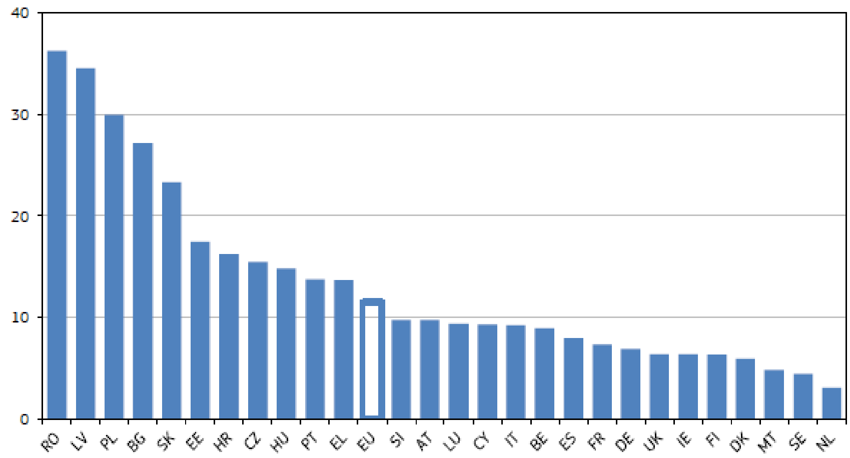

Figure 2. Pedestrian fatality rates per million population by country, European Union, 2013 [5]

3. PEDESTRIAN REGULATIONS

A pedestrian crash can usually be divided into 4 stages: the car initiate the contact with the pedestrian by touching his leg (tibia) with the front bumper, the frond edge of the bonnet or headlight hits the upper leg (pelvis), the head of the pedestrian hits the bonnet or the windshield, the pedestrian is projected in the air and hits the ground.
For the first three type of pedestrian impact are described in the European Commission Regulation, each using different sub-systems impactors to represent the main phases of a car-to-pedestrian impact.

ISSN 2457 – 5275 (Online, English)
ISSN 1842 – 4074 (Print, Online, Romanian)

The three types of impactors are:

- A legform impactor representing the adult lower limb to indicate lateral knee-joint shear displacement, bending angle and tibia acceleration, caused by the contact with the bumper
- A upper legform impactor representing the adult upper leg and pelvis to record bending moments and forces caused by the contact of the bonnet leading edge
- Child and adult headform impactors to record head accelerations caused by the contact with the bonnet

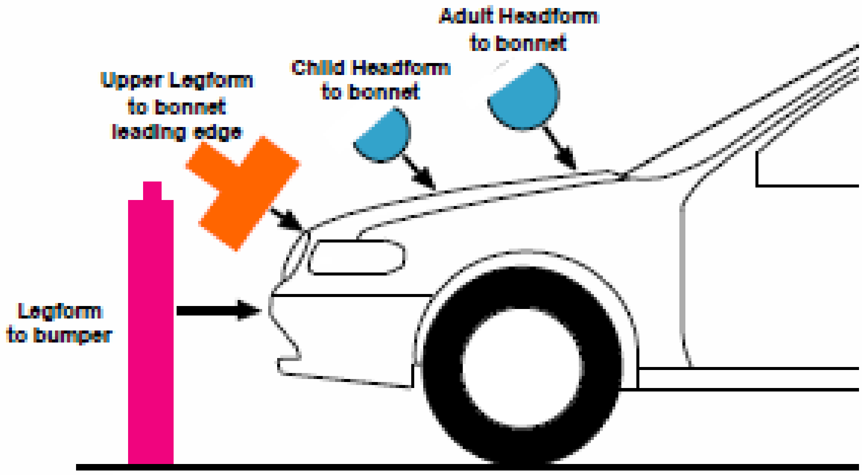

Figure 3. The sub-system tests used in EC directive [2]

A more exigent approach is conducted by the EuroNCAP program. The targets in this case are much lower and more criteria is analyzed during the physical tests. Also after the trial is conducted, each vehicle receives a score that finally contributes to the global rating of the car. Below is an example of the scoring configuration for EuroNCAP.

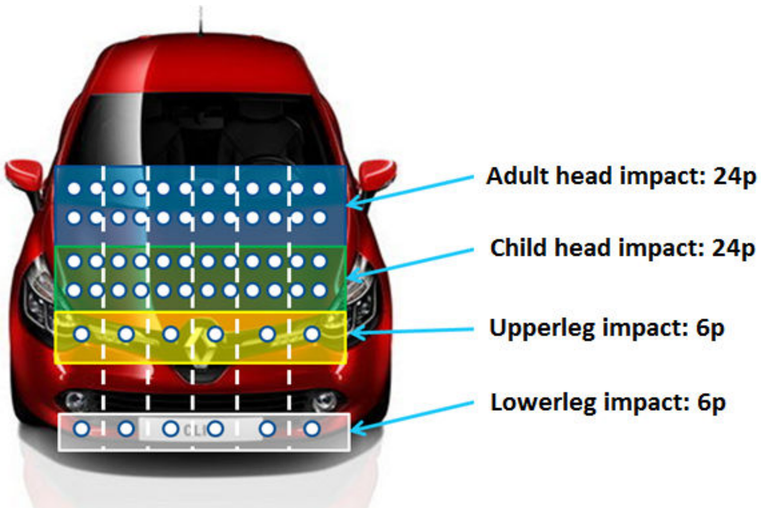

Figure 4. EuroNCAP scoring configuration

4. PEDESTRIAN FINITE ELEMENT SIMULATION

For researching the pedestrian impact it was used a finite element model composed of a simple front beam made from steel with a thickness of 1mm. It were launched two simulations to evaluate the difference in behavior between a classic solution of body in white front end and a modern one.
The impactor used for this trial consists of a metal center beam surrounded by two sheets of foam.
The total mass of the striker is calibrated to 9.5kg, as the EC directive describes.
The imposed initial speed was set at 40km/h and the impactor guided along X axis.

ISSN 2457 – 5275 (Online, English)
ISSN 1842 – 4074 (Print, Online, Romanian)

The results that will be analyzed are the force that is measured in the contact between the impactor and the crossbeams and three section moments (superior, center and inferior).
Requirements set to be respected by this type of test are 675daN for axial contact force and 450Nm for moment sections. The models used in simulation can be observed in the pictures below:

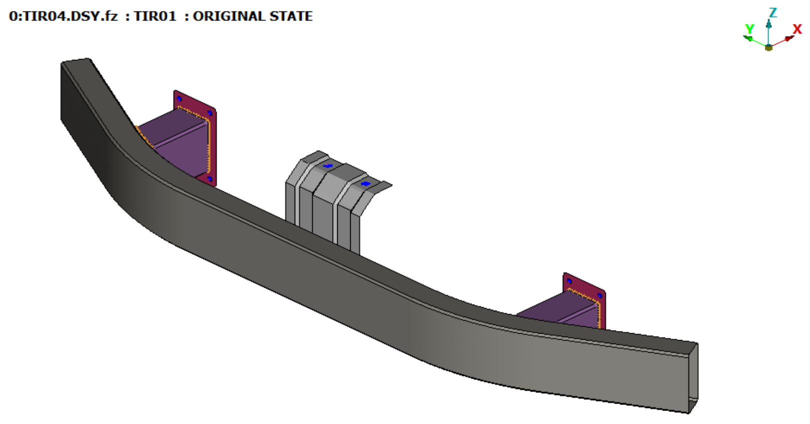

Figure 5. Classic crossbeam model

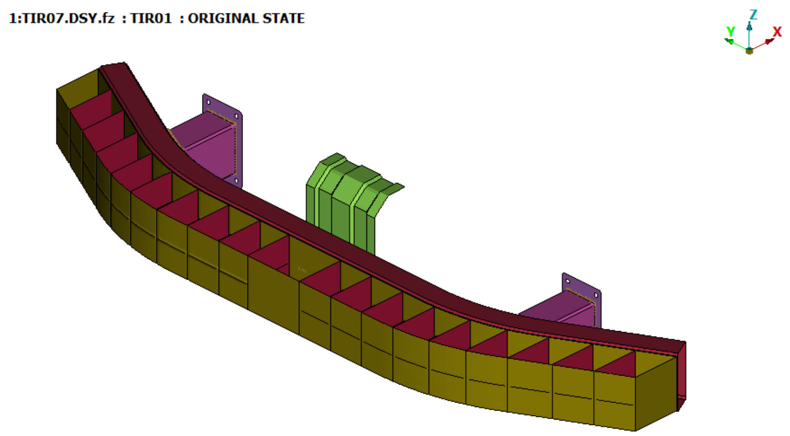

Figure 6. Modern crossbeam model (with shock absorber)

In the final state we can observe that the presence of the shock absorber reduces the risk of the legform hitting a hard structure component.
The maximum plastic deformations for the two models can be evaluated in the following pictures.

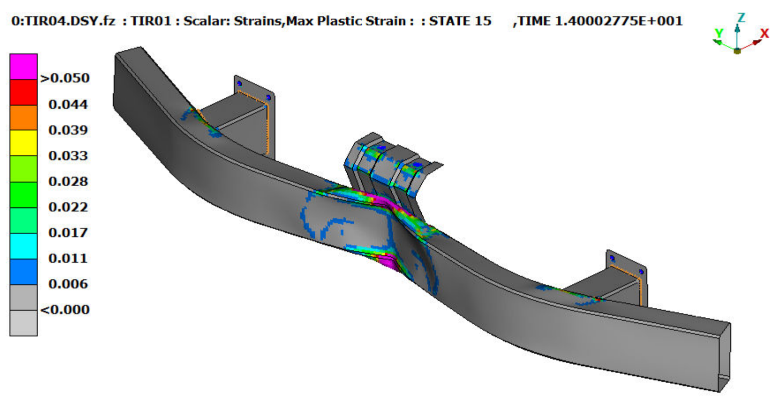

Figure 7. Classic crossbeam model – plastic deformation

ISSN 2457 – 5275 (Online, English)
ISSN 1842 – 4074 (Print, Online, Romanian)

In this case probably the pedestrian will be hardly injured.
Also the deformations of the structure in this case can lead to greater values of the forces and moments that are defined to be respected in the regulations.

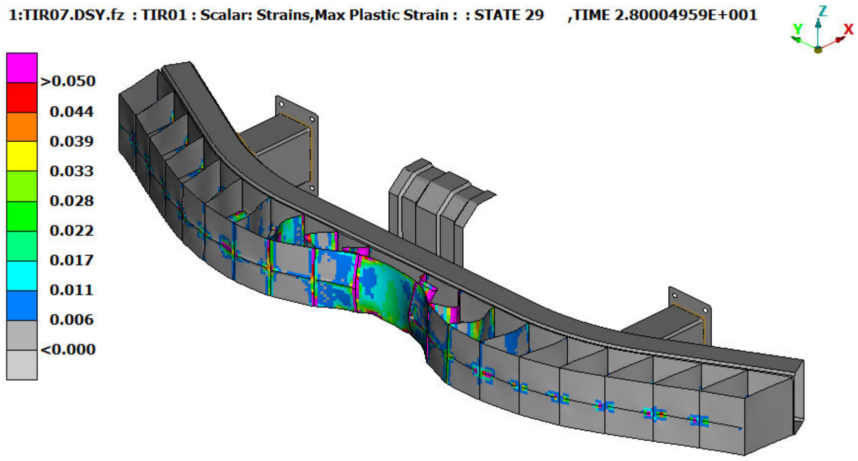

Figure 8. Modern crossbeam model – plastic deformation

The shock absorber has a good behavior and it manages to distribute the force to a greater surface of the crossbeam. Also, by deforming itself it absorbs a big part of the energy that does not reach the crossbeam.
The difference in deformation (mm) is very high between the two solutions, for the classic solution were identified 70mm in comparison with only 3mm measured for the modern configuration.
The values of the modern solution measured for the force and moments can be identified in the figure below. They don't exceed the limits imposed and are well distributed during the impact, assuring in this manner a good characteristic.

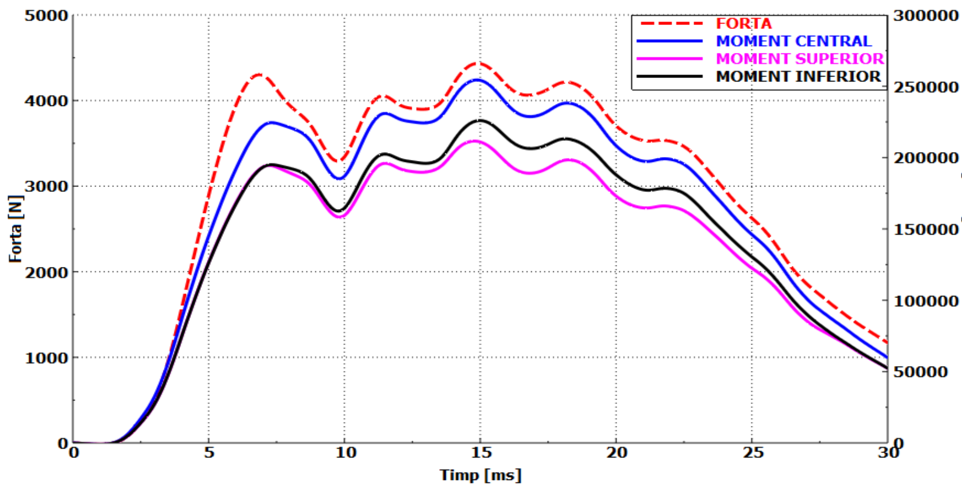

Figure 9. Modern crossbeam model – force and moment

5. CONCLUSION

The exigencies of the pedestrian regulations are constantly increasing worldwide, by imposing greater objectives by institutions like GlobalNCAP, EuroNCAP or NHTSA.
This fact has a huge impact over the future of automotive design, the front bumper being an element that is always reshaped in order to comply with the challenging architecture of the vehicle.

ISSN 2457 – 5275 (Online, English)
ISSN 1842 – 4074 (Print, Online, Romanian)

This paper offers a very fast calculation alternative for numerical simulation with the help of a simplified model, allowing to optimize quickly the volume available for a front bumper absorber in order to comply with the actual requirements. The results show good correlation in terms of deformation and values obtained for moments and forces. For future work, it is very important to compare the shape of the curves and the overall values with the full-scale physical model results.

This work was presented at the International Congress of Automotive and Transport Engineering CONAT 2016, Brasov, Romania and it was published in Proceedings of the Congress (ISSN 2069-0401).

REFERENCES

[1] Directive 2003/102/EC of the European Parliament and of the council of 17th November 2003.

[2] G.J.L Lawrence, J.A. Carrol, W.M.S. Donaldson, C. Visvikis, D.A. Peel , *A study on the feasibility of measures relating to the protection of pedestrians and other vulnerable road users* – Final report, EC Contract no FIF 20030937, TRL Limited, 2004.

[3] Rikard Fredriksson, *Priorities and potential of pedestrian protection. Accident data, experimental tests and numerical simulations of car-to-pedestrian impacts*, Karolinska Institutet, Stockholm 2011.

[4] F. A. Berg, M. Egelhaaf (Dekra Automobil GmbH), J. Bakker, H. Burke, R. Hermann, J. Scheerer, *Pedestrian protection in Europe. The potential of car design and impact testing*. (DaimlerChrysler AG) Germany 2010.

[5] *Traffic safety basic facts 2015 – Pedestrians*. European Road Safety Observatory Report, European Union, 2015.

[6] P. Schuster, *Current trends in bumper design for pedestrian impact,* SAE, 2006.

[7] E. Burnaz, A. Giubalca, *Pedestrian crash – Leg/Front bumper analysis*, Renault Technologie Roumanie, The annals of Dunarea de jos University of Galati, Fascicle V, Technologies in machine building, 2009.

RoJAE
Romanian
Journal of Automotive Engineering

AIMS AND SCOPE

The Romanian Journal of Automotive Engineering has as its main objective the publication and dissemination of original research in all fields of „Automotive Technology, Science and Engineering". It fosters thus the exchange of ideas among researchers in different parts of the world and also among researchers who emphasize different aspects regarding the basis and applications of the field.

Standing as it does at the cross-roads of Physics, Chemistry, Mechanics, Engineering Design and Materials Sciences, automotive engineering is experiencing considerable growth as a result of recent technological advances. The Romanian Journal of Automotive Engineering, by providing an international medium of communication, is encouraging this growth and is encompassing all aspects of the field from thermal engineering, flow analysis, structural analysis, modal analysis, control, vehicular electronics, mechatronics, electro-mechanical engineering, optimum design methods, ITS, and recycling. Interest extends from the basic science to technology applications with analytical, experimental and numerical studies.

The emphasis is placed on contribution that appears to be of permanent interest to research workers and engineers in the field. If furthering knowledge in the area of principal concern of the Journal, papers of primary interest to the innovative disciplines of „Automotive Technology, Science and Engineering" may be published.
No length limitations for contributions are set, but only concisely written papers are published. Brief articles are considered on the basis of technical merit. Discussions of previously published papers are welcome.

Notes for contributors
Authors should submit an electronic file of their contribution to the ***Production office:*** www. siar.ro. All the papers will be reviewed and assessed by a series of independent referees.

ISSN 2457 – 5275 (Online, English)
ISSN 1842 – 4074 (Print, Online, Romanian)

ISSN 2457 – 5275 (Online, English)
ISSN 1842 – 4074 (Print, Online, Romanian)

RoJAE
Romanian Journal of Automotive Engineering

The Scientific Journal of SIAR
A Short History

The engineering of vehicles represents the engine of the global development of the economy.
SIAR tracks the progress of the automotive engineering in Romania by: the development of automotive engineering, the development of technologies, and road transport services; supporting the work of the haulers, supporting the technical inspection and of the garage; encouraging young people to have a career in the automotive engineering and road haulage; stimulation and coordination of activities that promote an environment that is suitable for continuous education and improving of knowledge of the engineers; active exchange of ideas and experience, in particular for students, master students, PhD students, and young engineers, and dissemination of knowledge in the field of automotive engineering; cooperation with other technical and scientific organizations, employers' and socio-professional associations through organization of joint actions, of mutual interest.
By the accession to FISITA (International Federation of Automotive Engineering Societies) since its establishment, SIAR has been involved in achieving an overall professional community that is homogeneous in competence and performance, interactive, dynamic, and competitive at the same time, oriented towards a balanced and friendly relationship between people and the environment; this action will be constituted as a challenge worthy of effort and recognition.
The insurance of a favorable framework for the initiation and the development of cooperation of the specialists in this field of activity allows for an efficient and easy exchange of information, specific knowledge and experience; it supports the cooperation between universities and between research centers and industry; it speeds up the process of implementing the new technologies, it simplifies the identification of training and specialization needs of the personnel involved in the engineering of motor vehicles, transport, and road safety.
In order to succeed, ever since its founding, SIAR has considered that the stress should be put on the production and distribution, at national and international level, of a publication of scientific quality.

Under these circumstances, the development of the scientific magazine of SIAR had the following evolution:

1. RIA – Revista inginerilor de automobile (in English: ***Journal of Automotive Engineers***)
ISSN 1222 – 5142
Period of publication: 1990 – 2000 | Format: print, Romanian
Frequency: Quarterly | Electronic publication on: www.ro-jae.ro
Total number of issues: 30 | Type: Open Access
The above constitutes series nr. 1 of SIAR scientific magazine.

2. Ingineria automobilului (in English: ***Automotive Engineering***)
ISSN 1842 – 4074
Period of publication: as of 2006 | Format: print and online, Romanian
Frequency: Quarterly | Electronic publication on: www.ingineria-automobilului.ro
Total number of issues: 44 (including the September 2017 issue) | Type: Open Access
The above constitutes series nr. 2 of SIAR scientific magazine (Romanian version).

3. Ingineria automobilului (in English: ***Automotive Engineering***)
ISSN 2284 – 5690
Period of publication: 2011 – 2014 | Format: online, English
Frequency: Quarterly | Electronic publication on: www.ingineria-automobilului.ro
Total number of issues: 16 (including the December 2014 issue) | Type: Open Access
The above constitutes series nr. 3 of SIAR scientific magazine (English version).

4. *Romanian Journal of Automotive Engineering*
ISSN 2457 – 5275
Period of publication: from 2015 | Format: online, English
Frequency: Quarterly | Electronic publication on: www.ro-jae.ro
Total number of issues: 10 (September 2017) | Type: Open Access
The above constitutes series nr. 4 of SIAR scientific magazine (English version).

Summary – on September 30, 2017

Total of series:	*4*
Total years of publication:	*23 (11=1990 – 2000; 12=2006-2017)*
Publication frequency:	*Quarterly*
Total issues published:	*74 (Romanian), out of which, the last 27 were also published in English*

SIAR
Societatea Inginerilor de Automobile din România
Society of Automotive Engineers of Romania
www.siar.ro
www.ro-jae.ro